Reconstruction of short-term storm surge-driven increases in shallow coastal lake salinity using ostracod shell chemistry

Roberts, L.R.[1,2,3*], Holmes, J.A.[3], Horne D.J.[2], Leng M.J.[4,5], Sayer, C.D.[3], Timms R.G.O[6,7]., Flowers, K[6]., Blockley, S.P.M.[6] and Kelly, A.[8]

[1] Department of Ecoscience, Aarhus University, C. F. Møllers Allé 4-5, 8000 Aarhus, Denmark

[2] School of Geography, Queen Mary University of London, Mile End Road, London, E1 4NS, UK

[3] Environmental Change Research Centre, Department of Geography, University College London, Gower Street, London, WC1E 6BT, UK

[4] National Environmental Isotope Facility, British Geological Survey, Keyworth, Nottingham, NG12 5GG, UK

[5] Centre for Environmental Geochemistry, School of Biosciences, University of Nottingham, Sutton Bonington Campus, Loughborough, LE12 5RD, UK

[6]Centre for Quaternary Research, Department of Geography, Royal Holloway, University of London, Egham, Surrey, TW20 0EX, UK

[7]School of Archaeology, Geography and Environmental Science, University of Reading, Reading, RG6 6AB, UK

[8] Broads Authority, Yare House, 62-64 Thorpe Road, Norwich, NR1 1RY, UK

*Correspondence: l.roberts@ecos.au.dk

Abstract (max. 250 words)

Climate change threatens the current protection provided by coastal defences in low-lying mid-latitude regions and increases the risk to coastal lakes from future frequent and intense storms. Quantifying and understanding the impacts of past storm surges therefore has significant implications for the management and conservation of coastal wetlands worldwide. However, short-term (<10 year) increases in salinity driven by storm surges are problematic to reconstruct via the palaeolimnological record due to sampling resolution and smoothing of trends. Here, we propose that the geochemistry (Sr/Ca and $\delta^{18}O$) of calcitic shells of ostracods (small bivalved crustaceans readily preserved in lacustrine sediments) is a potentially sensitive proxy for reconstructing salinity, in some cases quantitatively, in comparison with sedimentary proxies of allochthonous sediment inputs (XRF and grain size) or other biological proxies. The coastal lakes of the Thurne Broads (Norfolk and Suffolk Broads National Park) in East Anglia UK, have a long history of sea floods associated with storm surge events in the North Sea, providing a test bed to compare ostracod palaeosalinity reconstructions (using a site-specific calibration) with known storm surges in the region. We show that Sr/Ca_{shell} values closely match known salinity changes associated with storm surges; archival records of the salinity of Horsey Mere in CE 1940 suggest a maximum salinity of 13.4 PSU with ostracod Sr/Ca_{shell} palaeosalinity calibrations giving a maximum value of 18.3 PSU. Ostracod shell chemistry therefore has the potential to afford more reliable reconstructions of high intensity short-term increases in salinity in mid-latitude low-lying coastal lakes.

Keywords: *Cyprideis torosa*; ostracods; oxygen isotope; Sr/Ca; coastal lakes; storm surge; salinisation

1. Introduction

With projected sea-level rise and increases in the frequency and intensity of storms, a primary concern for the conservation of coastal lakes, lagoons and wetlands is potential flooding of brackish or freshwater lakes with saline water. Periodic increases in salinity can affect the overall ecological functioning of coastal wetlands (see Herbert *et al*., 2015 for an overview) and, in some cases, can have economic consequences for local populations due to impacts on fisheries and agricultural irrigation (Damania *et al*., 2019). Knowledge of past flood events is of key importance for the assessment of likely future flooding. Instrumental and documentary records of flood history can be supplemented and verified by palaeolimnological records, which are valuable for reconstructing pre-industrial environmental change and can be used to reconstruct a range of climatic and anthropogenic stressors (Battarbee and Bennion, 2011). However, beyond the instrumental record, reconstructing periodic short-term (<10 years) increases in salinity has proven problematic due to the low temporal resolution and smoothing of trends in palaeolimnological studies.

The geochemistry and grain size of sedimentary archives have been commonly used to identify high-intensity flooding events (e.g. Liu *et al*., 2014; Chagué-Goff *et al*., 2016), but these often give limited direct and quantitative salinity data and fail to inform on the ecological recovery of lakes. Shifts in the presence, absence, abundance, and geochemistry of biological indicators, however, have the potential to give a more comprehensive reconstruction of salinity. Diatoms have regularly been used to reconstruct past salinity change from sediments (e.g. Espinosa 1994; Garcia-Rodriguez *et al*., 2004; Ryves *et al*., 2004; Tibby *et al*. 2007; Saunders, 2011; Witkowski *et al*., 2017), but the seasonality that is represented by diatom-inferred salinity is largely unknown (Reid *et al.,* 2002; Gell *et al.,* 2002), and in many cases diatom-salinity inference models can be affected by other co-varying environmental controls (e.g. pH change or nutrient enrichment). Short-term changes in salinity driven by extreme events have, therefore, been difficult to reconstruct accurately in mid-latitude lakes. Ostracod (small bivalved crustaceans readily preserved in lacustrine sediments) faunal assemblages and shell chemistry have, however, been used to identify short-term events such as tsunamis or hurricanes (e.g. Park *et al.*, 2009; Palmer *et al.,* 2020) and/or the freshening of lakes associated with increased storm precipitation (e.g. Lane *et al.*, 2017). Gouramanis *et al.* (2020) provide an overview of the use of ostracods in coastal overwash deposits of this type. In many cases, these studies are associated with large in-washing and deposition of coastal material, resulting in substantial shifts in sediment grain size and the introduction of marine taxa. In some circumstances, however, low-lying areas can experience storm surge flooding without high levels of sediment deposition seen after tropical storms, resulting in the requirement for proxies sensitive to short-term high-intensity increases in salinity.

There is good potential for the trace-element (Sr/Ca) and oxygen isotope ($\delta^{18}O$) geochemistry of calcitic shells of ostracods to reconstruct short-term increases in salinity because: 1) the shells calcify within a few hours to days providing a 'snapshot' of conditions; 2) in some circumstances it is possible to analyse multiple single valves within a stratigraphic interval, providing a measure of the variability in reconstructed parameters over a given time-period and; 3) there is good understanding of the life-cycle and therefore seasonality of many routinely-used ostracod species, for example the brackish water ostracod *Cyprideis torosa* (e.g. Heip, 1976; Horne, 1983).

The use of ostracod Sr/Ca_{shell} to reconstruct salinity follows the theory that the Sr content of ostracod shells is positively correlated with the Sr in lake water, which, in some circumstances, correlates with salinity (Chivas *et al*., 1985; De Deckker and Forester, 1988; Holmes and Chivas, 2002). Despite evidence for a small temperature dependence of Sr partitioning in *C. australiensis*, the Sr content of the shells is determined primarily by the Sr/Ca of the water (De Deckker *et al.,* 1999). In addition, the $\delta^{18}O$ is determined by water temperature and water-isotope composition, along with any vital effects (considered to be up to +3 ‰ depending on taxa; Xia *et al.,* 1997; von Grafenstein *et al*., 1999; Chivas *et al*., 2002; Keatings *et al*., 2002; Decrouy *et al*., 2011). In combination, the Sr/Ca and $\delta^{18}O$ theoretically allow a highly sensitive reconstruction of salinity; $\delta^{18}O_{shell}$ is a potentially more accurate record of periods of higher salinity due to the linearity of the $\delta^{18}O_{water}$ relationship with salinity in a freshwater/marine mixing model compared with the non-linear relationship between Sr/Ca_{water} and salinity (Anadón *et al*., 2002).

The East Anglian coastline of the UK (Fig. 1) has a long history of flooding associated with storm surge events in the North Sea (Hayman, 2012) with 23 floods recorded between 1287 and 2013 CE (all dates refer to Common Era throughout; Roberts *et al*., 2019). The comparatively shallow and restrictive southern basin of the North Sea funnels and constrains high water generated by eastward-tracking mid-latitude cyclonic systems, increasing sea level and making the east coast of the UK and west coast areas of mainland Europe particularly susceptible to storm surges (Spencer *et al*., 2015). When these storm surges coincide with high spring tides, there is high potential for extreme damage to low-lying coastal areas. For example, the 1953 flood resulted in the loss of over 300 lives in the east coast of England (Prichard, 2013). Following the flood, a concrete sea wall was erected, but despite considerable inter-annual variability, the general predicted trend is for North Sea storm surge activity to become more extreme by the end of the 21st century (Lowe *et al.*, 2001; Woth *et al*, 2005; Weisse *et al*., 2012; Dawson *et al.,* 2015). Furthermore, under a 'high' climate change scenario, sea level rise of the North Sea is predicted at 71 cm by 2050 and 107 cm by 2080, referenced to 1990 levels (Dawson *et al*., 2015). The current 1 in 100-year defence standard for eastern England, could be reduced to 1 in 2-8 years by 2050 and below the 1 in 1 year standard by 2080 (Nicholls and Wilson, 2002).

The coastal lakes of the Broads National Park (Fig. 1) support a range of ecosystem services (e.g. flood protection, provision of food, recreation, tourism and education; Natural England, 2009; Broads Authority, 2017) as well as being nationally and internationally important for nature conservation. The Thurne Broads system (Fig. 1), which lies closest to the North Sea coast, is designated as a Site of Special Scientific Interest (SSSI), Special Protected Area (SPA), Special Area of Conservation (SAC) and is protected under the Ramsar convention, as part of the Broadland Ramsar site. The surrounding landscape is dominated by reedbeds, fens and drained marshes. The Thurne Broads are naturally brackish lakes, affected by saline groundwater and seepage from the deepening of the drainage network (Holman and Hiscock, 1993; Fig. 1). In addition, Horsey Mere, which has no freshwater riverine inflow and is located <10 km from the North Sea coast, has experienced severe inundation from North Sea floods (Fig. 2) and the ecological impacts have been well documented, particularly following the 1938 flood (e.g. Buxton, 1939; Vincent, 1941; Ellis, 1944). Using documentary and palaeolimnological evidence to understand future threats from storm surge flooding is therefore of great importance to the local economy and to nature conservation on a local to international scale. The lakes are an ideal testbed for the use of ostracod shell chemistry to reconstruct short-term storm surge-driven increases in salinity because: 1) the storms and the ecological impacts on the coastal lakes of the Norfolk and Suffolk Broads are well documented (see Roberts *et al*., 2019 for an overview), providing ideal evidence to calibrate recent ostracod-based storm surge reconstructions of the North Sea; 2) previous work by Holmes *et al.* (2010) in the Thurne Broads has established a quantitative relationship between modern

C. torosa Sr/Ca_{shell} and water conductivity, allowing quantitative reconstructions of salinity; 3) sand layers and the sedimentary geochemical fingerprint associated with the 1953 flood have been recorded in saltmarsh cores along the Norfolk coast (Swindles *et al*., 2018); and 4) a storm precipitation/lake water mixing model corroborates that the salinity of the lake would not be affected by increased meteoric water (supplementary information 1). Here, we assess the sensitivity of Sr/Ca_{shell} and $\delta^{18}O_{shell}$ for reconstructing storm surges by combining ostracod-based reconstructions of salinity with sedimentary proxies of allochthonous sediment inputs (XRF and grain size) and calibrate them to known sea floods in the region.

2. Methods

2.1 Core recovery and chronology

A 43 cm Big Ben (Patmore *et al.*, 2014) core (HORSEY6) was collected from the eastern corner of Horsey Mere (Fig. 1) in September 2015 and sub-sampled at 0.5 cm resolution. Due to low unsupported ^{210}Pb and a truncated chronology, which is a common phenomenon in eutrophic shallow lakes, extrapolated ^{210}Pb dates were verified using the Spheroidal Carbonaceous Particles (SCPs) profile and, where possible, precise isochrons derived from tephrochronology.

Dried sediment samples from core HORSEY6 were analysed for ^{210}Pb, ^{226}Ra, ^{137}Cs and ^{241}Am by direct gamma assay in the Environmental Radiometric Facility at University College London (UCL), using an ORTEC HPGe GWL series well-type coaxial low background intrinsic germanium detector. ^{210}Pb was determined via its gamma emissions at 46.5keV, and ^{226}Ra by the 295keV and 352keV gamma rays emitted by its daughter isotope ^{214}Pb following 3 weeks storage in sealed containers to allow radioactive equilibration. ^{137}Cs and ^{241}Am were measured by their emissions at 662keV and 59.5keV (Appleby *et al.*, 1986). The absolute efficiencies of the detector were determined using calibrated sources and sediment samples of known activity. Corrections were made for the effect of self-absorption of low energy gamma rays within the sample (Appleby *et al*., 1992).

Analysis for SCPs followed the method described in Rose (1994). Reference concentrations agreed with the expected values at mean SCP concentration of 6005 ± 70 SCP per gram dry sediment (gDM^{-1}) and no SCPs were observed in the blanks. The start of the rapid increase in SCP concentration was assigned using the intercept of the extrapolated gradients of steady increase and the rapid increase (Rose *et al.*, 1995). Dates beyond the concentration peak of the SCP profile were assigned using the cumulative percentage data and the percentile dates described in Rose and Appleby (2005). For example, for Norfolk these have been assigned as 100 % 1970 ±5, 50 % 1955 ±5, 20 % 1910 ±20 and 1850 ±25 for the start of the record.

HORSEY6 was processed for cryptotephra following the stepped floatation method of Blockley *et al*. (2005). The core was examined for tephra presence at 0.5 cm resolution and samples containing tephra were counted using plane polarised light microscopy and presented as shards per gram of dry weight sediment. For geochemical analysis of cryptotephra from HORSEY6, shards were picked from samples under high-powered microscopy, using a gas chromatography syringe (Lane *et al*. 2014), mounted in epoxy resin, sectioned and polished. Major-element concentrations were determined using a Cameca SX-100 electron probe microanalyser at the University of Edinburgh. Beam diameter was set at 5 μm and at 15 keV. Beam current was set at 2 nA for Na_2O, Al_2O_3, SiO_2, FeO, K_2O, CaO, MgO and 80 nA for MnO, P_2O_5 and TiO_2 (Hayward, 2011). The microprobe was calibrated and assessed for accuracy and drift by the analysis of internal Lipari and BCR-2G standards.

2.2 Grain Size

Particle-size analysis was undertaken on the <2 mm fraction of sediment from samples at 0.5 cm intervals. Each sample was dispersed in water, sieved through a 2 mm mesh, and then disaggregated ultrasonically prior to analysis using a Malvern Mastersizer 2000 laser particle-sizer at UCL. The results were processed using GRADISTAT (Blott and Pye, 2001).

2.3 XRF

Concentrations of elements were measured on freeze-dried, milled samples of sediment samples at 0.5 cm intervals by X-Ray Fluorescence (XRF) spectroscopy using an Energy dispersive XRF (Bruker Ltd.) at UCL. The standard reference sediment Buffalo River (RM 8704) was prepared and run with the core samples, giving an average accuracy of ±10 %.

2.4 Ostracod and foraminifera faunal analyses

Around 5 cm^3 of core material was wet-sieved at 250 μm and the sample residue dried in an oven at 40 °C. Ostracod shells and foraminifera tests were picked under low-power stereo microscope using a 0000-paint brush, sorted and mounted on standard micropalaeontological slides, and identified using Meisch (2000) and Murray (1979) respectively. The total numbers of ostracod valves (adults and juveniles) and foraminifera tests per sample were counted and expressed as number of valves/tests per 10 cm^3. Ostracod assemblage zones (OAZs) were established using stratigraphically constrained cluster analysis by incremental sum of squares (CONISS) with the 'rioja' package in R (Juggins, 2020).

2.5 Ostracod shell chemistry

Additional single well-preserved adult or A-1 valves of *C. torosa* were picked for geochemical analysis; five valves were analysed for Sr/Ca and ten valves for $\delta^{18}O$. Soft tissue and any adhering dried sediment were removed from valves using needles, a fine paint brush wetted with methanol and ultra-pure 18.2Ω Milli Q deionised water under low-power stereo microscope. For trace element analysis, valves were then sonicated in methanol followed by 18.2Ω Milli Q deionised water and dried at 50 °C prior to analysis. For $\delta^{18}O$, valves were placed in in 500 µL of 15 % H_2O_2 for 15 minutes at room temperature in a 600 µL micro-centrifuge tube, rinsed with 18.2Ω Milli Q deionised water, and dried at 50 °C prior to analysis (Roberts *et al.*, 2018).

For trace metal analysis, single ostracod valves were dissolved in 500 µL of 1.07 M HNO_3 (trace metal grade) in an acid-leached (48h in 80 °C 10 % HNO_3) 600 µL micro-centrifuge tube. The Sr/Ca ratio of valves was determined using the intensity ratio calibration of de Villiers *et al*. (2002) using a Varian 720 ES ICP-OES at UCL. The results were corrected for blank intensity. Analysis of the carbonate standard BCS-CRM 393 gave an average Sr/Ca of 0.19 ±0.002 mmol/mol in agreement with the mean value of 0.19 mmol/mol quoted in Greaves *et al.* (2008).

Stable isotope analysis was undertaken on single valves using an IsoPrime dual inlet mass spectrometer plus Multiprep at the British Geological Survey. Isotope values ($\delta^{18}O$) are reported as per mille (‰) deviations of the isotope ratios ($^{18}O/^{16}O$) calculated to the VPDB scale using a within-run laboratory standard calibrated against NBS-19. The Craig correction was applied to account for ^{17}O. Analysis of the in-house standard calcite (KCM) gave good reproducibility of ±0.05 for $\delta^{18}O$.

2.6 Quantifying palaeosalinity

The partitioning of Sr into ostracod shells from the host water can be described as a K_D value using the following equation:

$$K_D[Sr] = Sr/Ca_{(shell)} / Sr/Ca_{(water)}$$

(1)

To determine palaeosalinity values, a site-specific K_D[Sr] value was determined using modern Sr/Ca_{water} and Sr/Ca_{shell} values from seasonal sampling of Horsey Mere in 2016 (N.B. a winter seasonal sample was not possible due to the overwintering of wildfowl). Determination of Sr/Ca_{shell} of modern ostracod shells followed the same analytical procedure as the downcore material described in section 2.5. Sr/Ca_{water} was analysed using a Varian 720 ES ICP-OES at UCL. Standards were prepared volumetrically using single element standard solutions of known concentrations. The results were corrected for blank intensity. Analysis of the standard river water SLRS-4 gave concentrations of 5.6 ±0.1 mg L^{-1} for Ca and 0.032 ±0.006 for Sr in good agreement with the published values of 6.2 mg L^{-1} for Ca and 0.026 mg L^{-1} for Sr (Yeghicheyan *et al.*, 2001).

At each interval downcore, the K_D value and equation (1) were then used to back-calculate Sr/Ca_{water} values for each individual (Sr/Ca_{shell} value), which was then used in the Thurne-specific palaeosalinity calibration of Holmes *et al*. (2010):

$$EC = ((4152717 * (Sr/Ca_{water}^{2}))) - (8883 * Sr/Ca_{water}) + 6.29$$

(2)

Due to the methods used in Holmes *et al*. (2010), equation (2) provides palaeosalinity values in electrical conductivity (mS cm^{-1}) and reconstructed salinity from Sr/Ca_{shell} values are therefore reported as EC throughout. However, other units of salinity are often reported in the literature with the salinity tolerance of ostracod species and monitoring or archival data more commonly reported in practical salinity units (PSU) or chloride concentration (mg/L). Electrical conductivity values were, therefore, converted to PSU following UNESCO (1983). In brief, if C(S,t,p) is EC of seawater at a known salinity (S), temperature (t) and pressure (p), the conductivity ratio is defined as:

$$R = C(S,t,p)/C(35,15,0)$$

(3)

Where C(35,15,0) is the EC of seawater at S 35, t 15°C and atmospheric pressure (p)

Archival records of salinity in chloride concentrations (mg/L), presented in detail in Roberts *et al*. (2019), were converted to PSU using Dauphinee (1980):

$$S = 0.0018066 * Cl$$

(4)

Since these conversions introduce further uncertainties in the reconstructed salinity values, the PSU value is reported alongside the original concentration or the reconstructed electrical conductivity value for comparison.

3. Results

3.1 Core chronology

Equilibrium of total ^{210}Pb activity with the supported ^{210}Pb in HORSEY6 occurred at ~15 cm. The unsupported ^{210}Pb profile had two sections; 1) the top 6.25 cm with little net decline in unsupported ^{210}Pb activities, suggesting an increase in sedimentation rates and 2) an irregular decline from 6.25 cm downwards, and rapidly declining to 0 from 14.25 cm, implying changes in sedimentation rates (Fig. 3a,b). There was a broad peak in ^{137}Cs activity between 10.25 and 14.25 cm (Fig. 3c), derived atmospheric fallout of nuclear weapons testing in 1963. The CRS dating model placed the 1963 depth at ~9 cm, which was considerably shallower than the depth suggested by the ^{137}Cs record. Radiometric chronologies of the core were corrected setting 1963 at 14.25 cm, as suggested by the ^{137}Cs record (Fig. 3d). Sedimentation rates in the core showed relatively small changes, and the mean sedimentation rate for the dated section of the core was 0.055 g cm^{-2} yr^{-1}.

The SCP profile for HORSEY6 shows a steady increase from 22 cm with rapid increase starting from ~17 cm (Fig. 4). There is a well-defined peak concentration of SCPs at 8 to 10 cm of 7,800 gDM^{-1}, followed by a decrease in concentrations to levels similar to the steady increase. The ^{210}Pb dates and SCP profile are in remarkable agreement for HORSEY6. The peak SCP concentration assigns 1970 ±5 at 10 cm in agreement with the ^{210}Pb assigned date of 1979 ±9. The 60th percentile places 1963 (1960 ±10) at 14 cm, the same interval as the ^{137}Cs peak assigned to 1963. Using the sedimentation rate of the last two radiometrically-dated increments gives a sedimentation rate that equates to 3.72 years per cm, giving a date of 1889 for the base of the core at 34.25 cm. This would assign 1850, and the start of the SCP profile, beyond the depth of the core. The SCP profile and cumulative percentile data places 1850 ± 25 at the base of the core, in good agreement with these dates despite the observed uneven sedimentation rate (Fig. 4). Using the difference between dates assigned by the SCP cumulative percentage (1940 ±15 at 16 cm, 1920 ±20 at 17 cm, 1910 ±20 at 18 cm and 1900 ±25 at 26 cm) to calculate extrapolated dates, and assuming an uncertainty of ±20 on extrapolated ^{210}Pb dates, there is good agreement between the SCP and radiometric dating methods.

Tephra shard peaks were recorded at 2 and 20 cm (Fig. 4). Shards at 2 cm are possibly representative of the 2010 eruption of Eyjafjallajökull, based on the age assigned by the ^{210}Pb age model. However, during analyses of the picked fraction the sample did not yield good results with acceptable analytical totals, which may be related to small shard size. A small number of shards from the 20 cm fraction did result in tephra chemistry with good analytical totals (Table 1). The geochemistry of the tephra shards at 20 cm is consistent with those published for Hekla 1947 (e.g. Larsen *et al.*, 1999; Housley *et al.*, 2010; Rea *et al.*, 2012; supplementary information 2). The geochemistry suggests a dacitic or rhyolitic eruption, forming pumice and therefore with low MgO and FeO and high SiO_2 (Savov *et al.*, 2008). While the comparison is limited by the small shard size and low shard numbers meaning it is difficult to compare the HORSEY6 shards across the range of expected compositions for Hekla 1947, there is a good match to Hekla 1947 on all element ratios and is a better match than other late Holocene widespread tephra, Askja 1875 (supplementary information 3). Moreover, the tephra at 20 cm coincides with the rapid increase in SCP concentration confirming the likelihood that the tephra is from the Hekla 1947 fallout. Hekla 1947 tephra has been found to coincide with a rapid increase in SCPs at a number of sites in Ireland (Rea *et al.*, 2012). Previous occurrence of Hekla 1947 tephra is known for North-East (Newcastle) and North-West (Lake District) England (Rea *et al.*, 2012). The presence of Hekla 1947 tephra in Norfolk hence extends the known dispersal of the ash cloud further south. Despite some uncertainty surrounding sediment accumulation, the additional control afforded by SCP derived dates allows a chronology to be constructed for core HORSEY6 with some confidence. The best available chronology, combing the three dating methods, is presented in Table 2.

3.1 Grain size

Percentage sand varied from 2.3 % in ~1857 (33.25 cm) to 43.8 % in ~ 2014 (1.25 cm) (Fig. 5). ‘Very coarse’ sand was present in twelve stratigraphic intervals with peaks in % sand occurring in eight intervals across core length (Table 3). The % sand appears as a peak at 21.25 cm, but it is associated with a lower percentage than the other peaks at 27.3 %. However, it is the highest percentage of coarse sand throughout the core at 4.6 %. During periods of low % sand (< 3 %) in ~ 1906 (23.75 cm), ~1878 (29.75 cm), ~1857 (33.25 cm), silt accounts for ~80 % of the sediment (Fig. 5). The core consists of two sedimentary units; clay from 32.25 to 25.25 cm and organic lake muds from 25.25 to 0.25 (Fig. 5). The boundary between sediment units is not associated with any change in grain size.

3.2 XRF

Concentrations of selected elements are presented in Fig. 6. There was high variability in all elements between ~1987 until ~1998 (between 8.25 cm and 5.75 cm). Prior to this, there was a gradual increase in P, Cl, Fe, Cu, Br, and Na with a gradual decrease in all other elements. Between ~1975 (11.25 cm) and ~1977 (10.75 cm) there was a sharp decline in Mg, Al, Si, Cl, K, Ca, Ti, Fe and Na before returning to concentrations similar to those in ~1970 (12.25 cm).

3.3 Ostracod and foraminifera fauna

Ostracod shells were present in the uppermost 24 cm of HORSEY6, with eleven taxa identified. In order of decreasing abundance, they were: *Cyprideis torosa, Darwinula stevensoni*, *Candona angulata, Candona candida, Limnocythere inopinata*, *Cypria subsalsa, Sarscypridopsis aculeata*, *Cypria ophtalmica, Pseudocandona compressa, Cytheromorpha fuscata,* and *Herpetocypris reptans*. (Fig. 7). Two foraminifera species were also identified, namely: *Trochammina inflata* and *Jadammina macrescens*. Three ostracod assemblage zones (OAZs) were identified using cluster analysis by incremental sum of squares (Fig. 8). Abundance is reported in valves per 10 cm^3, but raw count data is presented in supplementary information 4.

OAZ 1 (~1863 to 1906, 32.25 to 23.25 cm; Fig 8) is characterised by dominance of foraminiferal tests and almost complete absence of ostracod valves. *Trochammina inflata* is present in high abundance (>100 tests per 10 cm^3) throughout OAZ 1, but gradually decreases through OAZ1, with *J. macrescens* present in ~1863 to ~1875 (32.25 to 30.25 cm). Ostracods were not present in the core until ~1904 (25.25 cm) with the first occurrence of *C. torosa*, albeit it in low abundance (<6 per 10 cm^3), coinciding with the deposition of organic lake muds (Fig. 5) By ~1905 (24.25 cm), there was low abundance (between 4 and 84 valves per 10 cm^3) of *C. torosa, L. inopinata* and *C. subsalsa*.

Ostracod abundance increased in OAZ 2 (~1907 to 1983, 22.25 to 8.25 cm; Fig 8) to 120-292 valves per 10 cm^3 at each interval, but with a decline in *T. inflata* and *J. macrescens.* There was one occurrence of *T. inflata* in OAZ 2 in ~1930 (17.25 cm) (<4 tests per 10 cm^3). During OAZ 2, *Cypria subsalsa* and *P. compressa* are at their most abundant. Ostracod diversity also increases with the first occurrence of several species, namely: *C. subsalsa, P. compressa, C. ophtalmica, C. fuscata C. angulata* and *C. candida.* In ~1970 (12.25 cm), there was an increase in all present species except *S. aculeata*, which decreased in numbers. In ~1970 there was also the only occurrence of *C. ophtalmica* and the first occurrence of *C. fuscata,* which was also present in ~1979 (10.25 cm; Fig 8). Although the concentrations were low at

2-10 valves per 10 cm^3. In ~1952 (15.25 cm), there was a single occurrence of *C. candida* and *H. reptans.*

Valve concentration of *C. torosa*, *D. stevensoni* and *C. angulata* increased in OAZ 3 (~1987 to 2015, 7.25 cm to 0.25 cm; Fig 8) and reached a peak in ~2003 (2.25 cm) of <960 valves per 10 cm^3. 2003 (2.25 cm) was the only period where *L. inopinata* was present in OAZ 3. *Sarscypridopsis aculeata* was absent from OAZ 3*. Cyprideis torosa* continued to dominate and increase in abundance. After a reduction in abundance in ~1953 (7.25 cm), the abundance of *Candona* sp. began to increase until ~2015 (0.25 cm). There was an additional occurrence of *J. macrescens* in ~2003 (2.25 cm), but at a low concentration (<5 tests per 10 cm^3).

3.4 Ostracod shell chemistry

Sr/Ca_{shell} varied between 1.98 mmol/mol in ~1906 (23.25 cm) and 0.90 mmol/mol in ~2004 (4.25 cm) (Fig. 8; note the circles represent each individual Sr/Ca_{shell} or $\delta^{18}O_{shell}$ value with the grey shaded area representing the variability of shell values within the given stratigraphic interval, not an analytical error margin). There is a large step change in minimum Sr/Ca_{shell} values from >1.1 mmol/mol between ~1905 and 1915 (24.25 to 19.25 cm) to <1.0 mmol/mol from ~1920 to 2015 (18.25 to 0.25 cm) (Fig. 8). Peaks in Sr/Ca_{shell} occurred in ~1906 (23.25 cm) at 1.98 mmol/mol, between 1910 and 1915 (20.25 and 19.25 cm) at 1.74 and 1.72 mmol/mol, in ~1940 (16.25 cm) at 1.71 mmol/mol, in ~ 1963 (14.25 cm) 1.71 mmol/mol, in ~1979 (10.25 cm) at 1.55 mmol/mol, in ~1996 (6.25 cm) at 1.26 mmol/mol and in ~2003 (1.25 cm) at 1.51 mmol/mol.

$\delta^{18}O_{shell}$ values varied between +1.27 ‰ in ~1905 (24.25 cm) and –4.57 ‰ in ~2000 (5.25 cm) (Fig. 8). The mean $\delta^{18}O_{shell}$ varied little throughout the core from –1.03 ‰ in ~1905 (24.25 cm) to –2.67 ‰ in 2015 (0.25 cm), with a standard deviation of ±0.72 ‰ (1 σ) throughout the core. There is an overall decrease in $\delta^{18}O_{shell}$ through time, but with a period of higher $\delta^{18}O_{shell}$ values between ~1950 and 1975 (15.25 and 11.25 cm) (Fig. 8). Top-bottom comparisons of the maximum $\delta^{18}O_{shell}$ showed a change from high $\delta^{18}O$, (+1.27 ‰) to a value of –1.86 ‰. Maximum $\delta^{18}O_{shell}$ values varied by ±0.83 ‰ (1 σ) throughout the core. Whilst there is no step-change in minimum $\delta^{18}O_{shell}$ value-s as with Sr/Ca_{shells}, the minimum $\delta^{18}O_{shell}$ values are more variable over short periods of time prior to ~1940 (16.25 cm). From ~1905 to 1940 (24.25 to 16.25 cm; Fig. 8) there are three periods with high minimum $\delta^{18}O_{shell}$ values in ~1908 (21.25 cm) at –2.61 ‰, in ~1920 (18.25 cm) at –2.40 ‰ and in ~1940 (16.25 cm) at –2.08 ‰. There are peaks in maximum $\delta^{18}O_{shell}$ values at several stratigraphic intervals. These peaks occurred between ~1905 and 1910 (24.25 to 23.25 cm) with maximum values of +1.27 ‰ and +0.20 ‰, ~1915 and 1920 (19.25 to 18.25 cm) at +0.45 ‰ and +0.17 ‰, ~1966 and 1974 (13.25 to 11.25 cm) at +0.00 ‰, +0.33 ‰ and +0.80 ‰, and in ~1991 (7.25 cm) at +0.50 ‰.

3.5 Quantification of Sr/Ca_{shell}

Modern Sr/Ca_{shell} values in Horsey Mere ranged from 1.87 to 2.26 mmol/mol as recorded in autumn and spring 2016 respectively, with Sr/Ca_{water} values ranging from 2.85 mmol/mol in spring to 4.60 mmol/mol in autumn (Table 4). To produce a site-specific K_D value, the average Sr/Ca_{shell} value of 2.10 mmol/mol and the average Sr/Ca_{water} value of 3.98 mmol/mol were used, giving a K_D[Sr] value of 0.528 ± 0.05, which is comparable to the value published by Marco-Barba *et al*., (2012) of 0.57 ± 0.25. Using the K_D[Sr] value and equation (2), Sr/Ca_{shell} values of core-top material give comparable conductivity readings to those measured in situ in 2016; field measurements ranged from 8.60 to 11.21 mS cm^{-1} with calculated values ranging from 4.51 to 9.06 mS cm^{-1}.

Reconstructed salinity values range from 3.21 mS cm^{-1} in ~2004 (4.25 cm) to 31.18 mS cm^{-1} in ~ 1906 (23.25 cm) (Table 5). The peaks in Sr/Ca_{shell} values identified in the previous section are associated with conductivity values of 31.18 mS cm^{-1} in ~1906 (23.25 cm), 22.06 and 21.49 mS cm^{-1} between 1910 and 1915 (20.25 and 19.25 cm), 29.66 mS cm^{-1} in ~1940 (16.25 cm), 16.05 mS cm^{-1} in ~1979 (10.25 cm), and 14.82 mS cm^{-1} in 2014 (1.25 cm; Fig. 8; Table 5).

4. Discussion

The palaeolimnological evidence presented here can be linked to a number of documented sea floods affecting the lakes of the Broads National Park. In combination, the results represent both long-term smoothed patterns and periodic short-term increases in salinity. The ostracod faunal assemblage is typical of oligohaline conditions with some brackish-water and brackish-tolerant species present. There are no periodic increases in abundance or introductions of more saline tolerant species, suggesting that the faunal assemblage is largely a response to background salinity, as opposed to events leading to increased salinity. Throughout the core (except in the lowest section which is barren of ostracods), there is an abundance of *C. torosa,* a typically brackish-water species that can tolerate a wide range of salinities from almost freshwater to fully marine and hypersaline (Meisch, 2000). Present in lower numbers are typically freshwater species tolerant of brackish salinities (*D. stevensoni*, *L. inopinata, C. candida, P. compressa*, and *H. reptans*) as well as three with preferences for low-salinity brackish waters (*C. angulata*, *C. subsalsa* and *S. aculeata*; Meisch, 2000). The salinity tolerances of species present are in Table 6. The maximum salinity, based on the tolerance of the species present, is 14 PSU, with a period between ~ 1930 and 1979 (20.25 cm and 10.25 cm) of sustained raised salinity between 5 and 13.4 PSU. Higher salinities in OAZ1 (~1863 to 1906; Fig 9) are indicated by presence of the foraminifera *T. inflata* and *J. macrescens* (tolerant of salinities from 15 to 35 PSU, i.e. brackish to fully marine; Hayward and Hollis, 1994) from ~1860 to 1891 (32.25 to 23.25 cm; Fig 9), which are the only fossil species not present in the modern-day system. Low abundance of ostracods in this section suggests conditions unfavourable for ostracod occurrence and/or preservation. Low abundance is associated with the clay sedimentary unit. Furthermore, the foraminifera present are agglutinated and, therefore, not susceptible to the same effects of dissolution as calcitic ostracod valves. The foraminifera species present are typical of saltmarsh environments (Horton, 1999) and suggest a shallower more saline, perhaps intertidal, environment. An environment below mean high water level, suitable for foraminifera but not ostracods, with periodic inundation and lower sediment accumulation may account for the lack of ostracod valves recovered from this section of the core. Our coring location in the north-east of Horsey Mere and the age of the base of the core (~1850 ± 25) coincide with the Horsey Enclosure Act of 1812 when the direct oceanic connection to the north-east corner of Horsey Mere was closed off, suggesting a reduction in salinity (hence the loss of foraminifera) post ~1800 and a change in the extent of the lake. Saltmarsh conditions in the Thurne Broads in the mid to late 1800s are also suggested by the presence of these foraminifera species in cores collected from Hickling Broad (Holmes *et al*., 2010).

Historical records of ostracod faunas collected from Horsey Mere in the 1860s include *Cyprideis torosa*, *Cytheromorpha fuscata*, *Darwinula stevensoni*, *Limnocythere inopinata* and *Sarscypridopsis aculeata* (names are revised according to modern usage; Brady and Robertson, 1870). Species characteristic of low salinity brackish water were evidently present in Horsey Mere in the 1860s as suggested by Brady and Robertson (1870) and the presence of ostracod shells in an unpublished core from Horsey Mere (HORSEY3). However, no ostracod shells were recovered from HORSEY6 older than ~1903 (Fig. 9); this may be evidence of post-depositional dissolution of ostracod shells. Although *Cytheromorpha fuscata* was recorded in the Norfolk Broads by Brady and Robertson (1870) and is recorded in HORSEY6 in ~1970, it was not subsequently found alive in Britain until 1990 when it was collected in the Thurne Broads in the river between Heigham Sound and Martham Broad (Boomer and Horne, 1991). The occurrence of *Cypria subsalsa* in the HORSEY6 core is particularly interesting because this species has rarely been recorded in Britain, most likely because it has been confused with *Cypria ophtalmica*, a common species of which *C. subsalsa* was at first thought to be a variety. Unpublished records of *C. subsalsa* in Norfolk include the collection of living specimens from Breydon Water (I. Boomer, pers. comm., 2022). In Belgium and the Netherlands, it has been found exclusively in coastal and inland brackish waters (Wouters, 1984; Meisch, 2000). Interesting as the records of Brady and Robertson (1870) are for comparison, no clear distinction was made between live and dead specimens, and it is possible that shells of some brackish water taxa were transported in by tidal flow. The collection of living ostracods during our field campaign was insufficient to establish the diversity of the present-day living ostracod fauna.

While the ostracod fauna gives a good indication of background salinity, it fails to highlight short-term increases in salinity associated with storm surges, probably due to the broad salinity tolerances of the species present. However, the ostracod shell chemistry appears to indicate periodic short-term raised-salinity events. Palaeosalinity was highest in ~1906 and ~1940 (19.4 and 18.3 PSU; Table 5), coinciding with the tidal breaches at Horsey Gap in 1907 and 1938 (Mosby, 1939; Bankoff, 2013). The peak in Sr/Ca_{shell} at 23.25 cm (1.98 mmol/mol, 31.18 mS cm^{-1}) is associated with the 1906 storm surge. Following this, there was a sustained period of raised salinity between 1910 and 1915 (20.25 and 19.25 cm; 1.74 and 1.72 mmol/mol, 22.06 and 21.49 mS cm^{-1}). Salinity values appear to decrease between ~ 1907 to ~1908 (22.25 cm to 21.25 cm) with an increase in very coarse sand and low abundance of brackish water ostracod species in ~1910 (20.25 cm; Fig. 9). The sedimentary geochemical fingerprint of the 1953 flood has been recorded in saltmarsh cores along the North Norfolk coast at Holkham and a temporary decrease in Cl concentration of Horsey Mere sediments in ~1910 (20.25 cm; Fig. 7) is consistent with storm sand deposits associated with the 1953 floods (Swindles *et al.*, 2018). It is likely, therefore, that there was a higher accumulation of sediment associated with storm in-wash and that salinity of the lake remained high following the storm of 1907.

An increase in salinity in ~1930 (17.25 cm), sustaining in part through to ~1979 (10.25 cm), is supported by the single occurrence of *T. inflata* (<4 tests per 10 cm^3) and increase in *C. subsalsa* in OAZ 2, and the presence of very coarse sand in ~1930 (17.25 cm) (Fig. 9). The peak in Sr/Ca_{shell}, and therefore reconstructed salinity, occurs in ~1940 (16.25 cm) at 29.66 mS cm^{-1} (18.3 PSU). Despite, a long-term and remarkably detailed record of past salinity for Horsey Mere, the 1938 flood was not directly captured by past measurements. However, measured lake-water salinity values for 1939 suggest an increase from pre-flood values to a maximum of 4,460 mg/L, with a peak in chloride concentration in 1940 of 7,400 mg/L (Roberts *et al.*, 2019); equivalent to 8.1 and 13.4 PSU. This would confirm the peak in Sr/Ca_{shell} at 16.25 cm to be associated with the North Sea storm surge of 1938. Cl concentration of sediments also increases during this period (Fig. 7). The presence of proxies suggesting an increase in salinity from ~1930 could be due to increased sediment accumulation, due to flooding or the deepening of the agricultural drainage network, that is not taken into account in the age model, making these sediments as older than they are, and/or a time delay in the calcification of ostracods recording increased salinity. The proxies in combination confirm that salinity was sustained for several years following the 1938 flood. Documentary evidence suggests that Horsey Mere was still affected by increased salinity until 1950 (Buxton, 1951). Taking dating uncertainties into account, the peak in Sr/Ca_{shell} 14.25 cm of 1.71 mmol/mol (21.02 mS cm^{-1}; 12.6 PSU) is likely associated with the 1953 sea flood (Fig. 9). Following this peak, there is a period of sustained higher $\delta^{18}O_{shell}$. The Sr/Ca_{shell} during this period is low (1.05 to 1.17 mmol/mol), which, in combination with higher $\delta^{18}O_{shell}$ values (0.00 to +0.80 ‰), likely suggests salinity values above ~5 PSU when the local Sr/Ca mixing line becomes non-linear. Salinity above this level is confirmed by the mutual salinity tolerance of present ostracod species (5-13.4 PSU). A peak in Sr/Ca_{shell} equivalent to salinity of 16.05 mS cm^{-1} (9.4 PSU) in ~1979 (10.25 cm) is associated with the flood of 1978. Fewer documentary and monitoring archives of the floods of 1953 and 1978 exist, however the floods are considered to have had less impact on the lakes. Indeed, palaeolimnological evidence suggests that the salinity of the lakes returned to pre-1930 concentrations within five years of the 1978 flood. In combination, the floods of 1938, 1953 and 1978 caused a sustained increase in salinity to about 5 PSU until the early 1980s. An increase in salinity following these flood events has also been suggested from paleolimnological records of Hickling Broad (e.g., Holmes *et al*., 2010), providing evidence of an increase in salinity occurring across the Thurne Broads.

The high variability in elemental concentration of sediments after ~1987 until ~1998 is likely linked to high variability in salinity (Fig. 9). Monitoring data for Horsey Mere suggest that the greatest annual variability in salinity was in 1994, ranging from 1,160 to 8,500 mg/L (2.1 to 15.4 PSU) (Roberts *et al*., 2019). The Sr/Ca_{shell} values suggest a range between 2.1 and 4.8 PSU with the variability in $\delta^{18}O_{shell}$ high in ~1991 (7.25 cm) at ±4.81 ‰ with a maximum value of +0.5 ‰. This again suggests periods of raised salinity above 5 PSU, and non-linearity of the Sr/Ca mixing line. There is very low abundance and diversity of ostracods with only *C. torosa* and *Candona* juveniles recorded in ~1991 suggesting increased salinity (Fig. 9). A tidal surge in 1993 (Kindleysides, 1993) is associated with some of this variability in salinity, but is likely a combination of the effects of storm surges and enhanced and deeper agricultural drainage system, resulting in groundwater ingress into the surrounding drainage network (drainage pumping locations are denoted by triangles in Fig. 1). For instance, the 1979 drainage scheme on the West Somerton Level resulted in a doubling of salinity in Martham Broad in the 1980s (Driscoll, 1984; George, 1992). It is likely, whilst not documented, that deep drainage impacted the other broads of the Thurne system. *Sarscypridopsis aculeata* was absent from OAZ 3 (~1987 to 2015, 8.25 cm to 0.25 cm), suggesting lower salinity overall and water ionic composition more similar to the freshwater end member. However, a peak in Sr/Ca_{shell} of 1.51 mmol/mol (14.82 mS cm^{-1}; 1.25 cm) coincides with the 2013 tidal surge (Eastern Daily Press, 2013). Taking into account uncertainties in dating and sediment accumulation, the presence of *J. macrescens* at 2.25 cm, but at a low concentration (<5 tests per 10 cm^3), is likely also associated with the 2013 tidal surge (Fig. 9).

5. Conclusions

Sr/Ca and $\delta^{18}O$ values of ostracod shells provide a sensitive proxy for understanding short-term increases in salinity associated with storm surges. Notwithstanding errors and uncertainties associated with intermittent monitoring and calibration studies, the Sr/Ca_{shell} values closely match known salinity changes associated with storm surges; archival records of the salinity of Horsey Mere in 1940 suggest a maximum salinity of 13.4 PSU with ostracod Sr/Ca_{shell} palaeosalinity calibrations giving a maximum value of 18.3 PSU. Due to a lack of regular monitoring during the 1930s, the previous most comprehensive archival and documentary reports of the floods of 1938 suggest that salinity had returned to previous levels within six years. Palaeolimnological evidence, however, suggests that increased salinity was sustained for up to ~40 years likely due to the frequency and intensity of floods and deepening of drainage during this period, resulting in a lack of recovery between floods and an increase in baseline salinity. Background salinity decreased in the 1970s due to protection from the Sea Palling sea wall, erected after the 1953 flood. However, the likely increased stress on sea walls due to continued climate change-related sea level rise and a predicted increase in extreme storms could result in future threats to the coastal lakes of Eastern England and other low-lying areas of Western mainland Europe. Quantifying and understanding the impacts of past storm surges will have significant implications for the management of locally, nationally, and internationally important sites of coastal conservation worldwide.

Acknowledgements

Figure 2 has been reproduced with the permission of Historic Environment England under the licence number EPW056554. The research was funded by a studentship from the UK Natural Environment Research Council as part of the London NERC DTP (NE/L002485/1) and a CASE partnership with the Broads Authority. The collection of modern samples from Horsey Mere was funded by a New Researcher's Award from the Quaternary Research Association. The authors thank: Robin Buxton and the National Trust for permission to sample Horsey

Mere; the UK Environment Agency for providing water quality monitoring data; Huw Bennett and Panagiotis Koullouros for processing of samples; Ian Boomer for providing specimens of *C. subsalsa* collected in Norfolk for comparison with our core material; Peter Doktor from the Environment Agency for insightful comments on the current Norfolk coastline coastal defences; Jim Davy for assistance with SEM imaging; and Miles Irving for cartography and figure drafting assistance.

List of Tables

Table 1. Horsey Mere WDS EPMA (University of Edinburgh) tephra chemistry major element oxide concentrations

Table 2. Chronology for HORSEY6 combining SCP, ^{210}Pb dates and tephrochronology

Table 3. Presence of very coarse sand and peaks in % sand in core HORSEY6

Table 4. Modern Sr/Ca_{water} and $Sr/Ca_{ostracod}$ values for Horsey Mere used to calculate a site-specific K_D value.

Table 5. Downcore $Sr/Ca_{ostracod}$ values, back-calculated Sr/Ca_{water} using the K_D value calculated in Table 4, and the reconstructed conductivity using the calibration of Holmes *et al*. (2010). Conductivity values are converted to PSU using UNESCO (1983). Reconstructions are for the period 2015-1905, after which *C. torosa* is not present in the core.

Table 6. Salinity tolerances of ostracod and foraminifera species present in core HORSEY6

List of figures

Figure 1. Location of the Upper Thurne Broads showing pump locations (denoted as triangles), settlements (in grey), the drainage network (in blue), and the coring location (grey circle). Adapted from Roberts *et al.* (2019)

Figure 2. Aerial imagery of flooding around Horsey Corner, located ~1 km north of Horsey Mere, after the 1938 North Sea storm surge. (Image © Historic England)

Figure 3. Fallout radionuclide concentrations in core HORSEY6 taken from Horsey Mere, Norfolk, showing a) total ^{210}Pb, b) unsupported ^{210}Pb, c) ^{137}Cs concentrations versus depth, and d) radiometric chronology of core HORSEY6, showing the CRS model ^{210}Pb dates and sedimentation rates. Zero is equivalent to the surface sediment in 2015

Figure 4. Dating profiles for Horsey Mere. Features used to define the chronology are highlighted for each profile of a) unsupported ^{210}Pb, b) ^{137}Cs, c) SCP concentration and d) cryptotephra horizons

Figure 5. Core log and sediment description plotted alongside grain size of sediments comprising core HORSEY6. Selected size fractions are shown expressed as % sediment type.

Figure 6. Geochemical stratigraphy of Horsey Mere. Selected elements are shown and expressed as concentration (ppm)

Figure 7. Scanning electron microscope images of selected ostracod and foraminiferal taxa from core HORSEY6 that are significant for estimation past salinity. All are external view. The 100 μm scale bar applies to images 1-2 and 4-9 and the 200 μm scale bar to image 3 only. Depths represent levels in HORSEY6 from which each specimen was recovered. 1. *Pseudocandona compressa,* female, adult, LV (10-10.5 cm); 2. *Cyprideis torosa,* male, adult, RV (2-2.5 cm); 3. *Candona angulata,* male, adult, LV (10-10.5 cm); 4. *Sarscypridopsis aculeata*, female, adult, LV (10-10.5 cm); 5. *Cypria ophtalmica*, female, adult, LV (12-12.5 cm); 6. *Cypria subsalsa,* lack of soft parts for identification but presumed female, adult, LV (12-12.5 cm); 7. *Cytheromorpha fuscata,* male, adult, RV (10-10.5 cm); 8. *Trochammina inflata* (32-32.5 cm); 9. *Jadammina macrescens* (32-32.5 cm)

Figure 8. Ostracod faunal assemblage and ostracod geochemistry for core HORSEY6. Dates are radiometrically determined until 1963 ±10 after which the italicised dates are based on the SCP profile, tephrochronology, and extrapolation**.** The grey shading represents the range of ostracod geochemical data within a stratigraphic interval, not an error margin.

Figure 9. Palaeolimnological data from core HORSEY6 allowing reconstruction of smoothed ‘background’ and periodic increases in salinity. Dates are radiometrically determined until 1963 ±10 after which the italicised dates are based on the SCP profile, tephrochronology, and extrapolation. The grey shading represents the range of ostracod geochemical data within a stratigraphic interval, not an error margin. Monitoring data of salinity (Chloride mg/L) is presented alongside the paleolimnological proxies of salinity: the mean values are denoted by the points and black line; the minimum and maximum values are denoted by the grey dashes.

Supplementary Information 1. Mixing model between storm precipitation (0 PSU) and Horsey Mere lake water (5.6 PSU). Storm precipitation as the proportion of lake water is calculated for the 2013, 1953, and 1938 storm surges. Monthly rainfall data were recorded at Lowestoft Meteorological Station (Met Office, 2022).

Supplementary Information 2. Total alkali-silica biplot of the HORSEY6 tephra at 20 cm (denoted by crosses) against the data for Icelandic eruptions from Hekla 1947 (denoted by triangles) and Askja 1857 (denoted by circles). Historical Icelandic tephra data are from the University of Edinburgh tephra database (http://www.tephrabase.org)

Supplementary Information 3. Variation plots of tephra chemistry major element oxide concentrations. Chemistry of HORSEY6 tephra is denoted by the green crosses with the red triangles and black dots denoting chemistry of widespread late Holocene tephras (Askja 1875 and Hekla 1947).

Supplementary Information 4. Ostracod and foraminifera faunal count data from HORSEY6

Table 1. Horsey Mere WDS EPMA (University of Edinburgh) tephra chemistry major elements oxide concentrations

Code	SiO_2	TiO_2	Al_2O_3	FeO	MnO	MgO	CaO	Na_2O	K_2O	P_2O_5	Total
HO 20.0-20.5	74.35	0.08	12.86	0.97	0.05	0.08	0.75	3.45	4.57	0.02	97.19
HO 20.0-20.5	71.74	0.07	12.59	0.96	0.05	0.08	0.95	3.35	4.27	0.37	94.43
HO 20.0-20.5	70.27	0.80	12.81	5.24	0.14	0.69	3.17	3.59	1.78	0.18	98.65

Table 2. Chronology for HORSEY6 combining SCP, ^{210}Pb dates and tephrochronology

Depth (cm)	Date CE	±
0	2015	
0.25	2014	2
2.25	2010	2
4.25	2004	4
6.25	1996	5
8.25	1987	7
10.25	1979	9
11.25	1974	11
12.25	1970	12
14.25	1963	15
16.25	1940	15
18.25	1920	20
20.25	1910	20
22.25	1907	
24.25	1905	
26.25	1900	25
28.25	1888	
30.25	1875	
32.25	1863	
34.25	1850	25

Table 3. Presence of very coarse sand and peaks in % sand in core HORSEY6

Approximate year	Core depth (cm)	Peaks in grain size	
		% very coarse sand	% sand
2014	1.25		43.8
2012	1.25	0.46	
2006	3.75		33.3
1989	7.75		40.7
1970	12.25	1.03	38.4
1976	13.25	0.28	
1935	16.75	0.04	
1930	17.25	0.44	
1915	19.25		31.2
1910	20.25	1.67	
1909	21.25	1.51	27.3
1897	16.75	4.45	
1888	28.25	0.15	
1879	26.75		33.8
1872	30.75	1.17	
1863	32.25	0.20	
1860	32.75		19.5
1857	33.75	0.60	

Table 4. Modern Sr/Ca_{water} and Sr/$Ca_{ostracod}$ values for Horsey Mere used to calculate a site-specific K_D value. Sampling between September and April for a winter Sr/Ca_{water} value was not possible due to the overwintering of wildfowl.

Date	**Sr/Ca_{water} (mmol/mol)**	**Spatial and Seasonal variation (1σ)**	**Analytical error**	**Sr/Ca_{shell} (mmol/mol)**	**Spatial and Seasonal variation (1σ)**	**Analytical error**	**K_D Value**
Apr-16	2.850	0.672	±0.006	2.263	0.140	±0.001	0.794
	3.038						
	4.339						
Jun-16	4.437			2.115			0.477
	3.451						
	4.339						
Sep-16	4.599			1.869			0.406
	4.314			2.198			0.510
	4.439			2.018			0.455
				2.142			0.483
Average	**3.978**			**2.101**			**0.528 ± 0.05**

Table 5. Downcore Sr/$Ca_{ostracod}$ values, back-calculated Sr/Ca_{water} using the K_D value calculated in in Table 4, and the reconstructed conductivity using the calibration of Holmes *et al*. (2010). Conductivity values are converted to PSU using UNESCO (1983).

	Sr/Ca$_{shell}$ (mmol/mol)			Sr/Ca$_{water}$ (mmol/mol)			Palaeosalinity (mS cm^{-1})			PSU		
Year	**Mean**	**Max**	**Min**	**Mean**	**Max**	**Min**	**Mean**	**Max**	**Min**	**Mean**	**Max**	**Min**
2015	1.11	1.28	1.01	2.1	2.41	1.91	5.96	9.06	4.51	3.2	5.1	2.4
2014	1.16	1.51	0.99	2.2	2.86	1.88	6.86	14.82	4.29	3.8	8.6	2.3
2010	1.23	1.23	1.23	2.32	2.32	2.32	8.04	8.04	8.04	4.5	4.5	4.5
2007	1.14	1.26	1.06	2.15	2.39	2.01	6.39	8.75	5.25	3.5	4.9	2.8
2004	1.04	1.19	0.90	1.97	2.26	1.70	4.91	7.41	3.21	2.6	4.1	under scale
2000	1.09	1.16	1.00	2.06	2.19	1.89	5.59	6.77	4.33	3.0	3.7	2.3
1996	1.15	1.26	1.05	2.18	2.38	1.99	6.62	8.64	5.09	3.6	4.8	2.7
1991	1.04	1.07	0.97	1.97	2.03	1.83	4.94	5.37	3.93	2.6	2.9	2.1
1987	1.07	1.18	0.98	2.03	2.24	1.85	5.35	7.23	4.05	2.9	4.0	2.1
1983	1.07	1.27	0.95	2.03	2.41	1.80	5.40	9.01	3.74	2.9	5.0	under scale
1979	1.25	1.55	1.05	2.37	2.94	1.98	8.61	16.05	5.00	4.8	9.4	2.7
1974	1.04	1.05	1.02	1.97	1.99	1.94	4.87	5.10	4.67	2.6	2.7	2.5
1970	1.11	1.16	1.06	2.10	2.20	2.02	5.94	6.88	5.26	3.2	3.8	2.8
1966	1.00	1.17	0.92	1.89	2.21	1.74	4.31	6.94	3.40	2.3	3.8	under scale
1963	1.17	1.71	1.02	2.22	3.24	1.93	7.03	21.02	4.62	3.9	12.6	2.5
1951	1.06	1.32	0.95	2.00	2.50	1.80	5.15	10.03	3.76	2.8	5.6	under scale
1940	1.3	1.94	0.94	2.46	3.67	1.77	9.56	29.66	3.6	5.4	18.3	under scale
1930	1.14	1.45	0.91	2.15	2.75	1.73	6.40	13.32	3.34	3.5	7.7	under scale
1920	1.26	1.39	1.00	2.39	2.63	1.90	8.78	11.71	4.41	4.9	6.7	2.3
1915	1.57	1.72	1.48	2.98	3.26	2.80	16.65	21.49	14.02	9.8	12.9	8.1
1910	1.37	1.74	1.15	2.59	3.29	2.18	11.12	22.06	6.68	6.3	13.3	3.7
1908	1.39	1.65	1.24	2.64	3.12	2.35	11.73	19.05	8.31	6.7	11.3	4.6
1907	1.39	1.61	1.15	2.64	3.06	2.18	11.76	17.96	6.62	6.7	10.6	3.6
1906	1.62	1.98	1.32	3.07	3.74	2.50	18.14	31.18	10.00	10.7	19.4	5.6
1905	1.42	1.76	1.12	2.69	3.34	2.12	12.43	22.99	6.09	7.1	13.9	3.3

Table 6. Salinity tolerances of ostracod and foraminifera species present in core HORSEY6

Species	Salinity tolerance (PSU)	Reference
Cyprideis torosa	0.4 to 150	Meisch, 2000
Darwinula stevensoni	Up to 15	Meisch, 2000
Sarscypridopsis aculeata	Up to 17.2 with an optimum of 5 to 10	Ganning, 1971; Henderson, 1990; Meisch and Broodbakker, 1993; Griffiths, 1995; Meisch, 2000; Holmes *et al*., 2007
Limnocythere inopinata	Up to 25	Neale, 1988; Löffler, 1990
Pseudocandona compressa	Up to 8.4	Hiller, 1972; Meisch, 2000
Candona angulata	0.2 to 14	Meisch, 2000
Candona candida	Up to 5.77	Hiller, 1972; Meisch, 2000
Cypria subsalsa	0.5 to 13.4	Meisch, 2000
Cypria ophtalmica	Up to 6	Delorme, 1978; Neale, 1988; Geiger, 1990; Meisch, 2000
Cytheromorpha fuscata	0.5 to 20	
Herpetocypris reptans	0.5 to 6	Yassini 1969; Usskilat, 1975
Trochammina inflata	15 to 35	Hayward and Hollis, 1994
Jadammina macrescens	15 to 35	Hayward and Hollis, 1994

References

Anadón, P., Gliozzi, E., & Mazzini, I. 2002. Palaeoenvironmental reconstruction of marginal marine environments from combined palaeoecological and geochemical analyses on ostracods. In J. A. Holmes & A. R. Chivas (Eds.), *The Ostracoda: applications in Quaternary research* (Vol. 131, pp. 227-247). Washington DC: American Geophysical Union.

Appleby, P. G., Nolan, P. J., Gifford, D. W., Godfrey, M. J., Oldfield, F., Anderson, N. J. & Battarbee, R. W. 1986. 210Pb dating by low background gamma counting. *Hydrobiologia,* 143**,** 21-27.

Appleby, P., Richardson, N. & Nolan, P. 1992. Self-absorption corrections for well-type germanium detectors. *Nuclear Instruments and Methods in Physics Research Section B: Beam Interactions with Materials and Atoms,* 71**,** 228-233.

Bankoff, G. 2013. The 'English Lowlands' and the North Sea Basin System: A History of Shared Risk. *Environment and History,* 19**,** 3-37.

Battarbee, R.W., Bennion, H. 2011. Palaeolimnology and its developing role in assessing the history and extent of human impact on lake ecosystems. *Journal of Paleolimnology* 45, 399–404.

Blockley, S. P. E., Pyne-O'donnell, S. D. F., Lowe, J. J., Matthews, I. P., Stone, A., Pollard, A. M., Turney, C. S. M. & Molyneux, E. G. 2005. A new and less destructive laboratory procedure for the physical separation of distal glass tephra shards from sediments. *Quaternary Science Reviews,* 24**,** 1952-1960.

Blott, S. J. & Pye, K. 2001. GRADISTAT: a grain size distribution and statistics package for the analysis of unconsolidated sediments. *Earth Surface Processes and Landforms,* 26**,** 1237-1248.

Boomer, I. & Horne, D.J. 1991. On *Cytheromorpha fuscata* (Brady). *A Stereo-Atlas of Ostracod Shells,* 18, 49-56.

Brady, G.S. & Robertson, D. 1870. Ostracoda and Foraminifera of tidal rivers. *The Annals and Magazine of Natural History,* Ser. 4, vol. vi, No. 31, pp.1-33, 308, pls IV-X.Broads Authority. 2017. *Broads Plan 2017: Partnership strategy for the Norfolk and Suffolk Broads*. Norwich, UK: Broads Authority.

Buxton, R. 1939. The Norfolk Sea Floods February, 1938 3. General effects of the flood. *Transactions of the Norfolk and Norwich Naturalists'* Society, *14*, 349-373
Buxton, R. 1951. Wild Bird protection in Norfolk in 1950. Report of the Council. *Transactions of the Norfolk and Norwich Naturalists' Society, 17*, 90-122.
Chagué-Goff, C., Chan, J. C. H., Goff, J. & Gadd, P. 2016. Late Holocene record of environmental changes, cyclones and tsunamis in a coastal lake, Mangaia, Cook Islands. *Island Arc,* 25**,** 333-349.
Chivas, A. R., De Deckker, P. & Shelley, J. M. G. 1985. Strontium content of ostracods indicates lacustrine palaeosalinity. *Nature,* 316**,** 251.
Chivas, A. R., De Deckker, P., Wang, S. X., & Cali, J. A. (2002). Oxygen-isotope systematics of the nektic ostracod *Australocypris robusta*. In J. A. Holmes & A. R. Chivas (Eds.), *The Ostracoda: applications in Quaternary research* (Vol. 131, pp. 301-313). Washingtson DC: American Geophysical Union.
Damania, R., Desbureaux, S., Rodella, A-S., Russ, J., & Zaveri, E. 2019. *Quality Unknown: The Invisible Water Crisis*. Washington, DC: World Bank.
Dauphinee, T. 1980. Introduction to the special issue on the Practical Salinity Scale 1978. *IEEE Journal of Oceanic Engineering, 5*(1), 1-2.
Dawson, R. J., Nicholls, R. J. & Day, S. A. 2015. The Challenge for Coastal Management During the Third Millennium. *Broad Scale Coastal Simulation.* Springer.
De Deckker, P. & Forester, R. 1988. The use of ostracods to reconstruct continental palaeoenvironmental records. In P. De Deckker, J.-P. Colin & J.-P. Peypouquet (Eds.) *Ostracoda in the earth sciences* (175-199). Amsterdam: Elsevier
De Deckker, P., Chivas, A. R. & Shelley, J. M. G. 1999. Uptake of Mg and Sr in the euryhaline ostracod Cyprideis determined from in vitro experiments. *Palaeogeography Palaeoclimatology Palaeoecology,* 148**,** 105-116.
De Villiers, S., Greaves, M. & Elderfield, H. 2002. An intensity ratio calibration method for the accurate determination of Mg/Ca and Sr/Ca of marine carbonates by ICP-AES. *Geochemistry, Geophysics, Geosystems,* 3.
Decrouy, L., Vennemann, T. W. & Ariztegui, D. 2011. Controls on ostracod valve geochemistry: Part 2. Carbon and oxygen isotope compositions. *Geochimica et Cosmochimica Acta,* 75**,** 7380-7399.
Delorme, L.D. 1978. Distribution of freshwater ostracodes in Lake Erie. *Journal of Great Lakes Research*, 4, 216– 220.
Driscoll, R. J. 1984. Chloride ion concentrations in dyke water in the Thurne Catchment area in 1974 and 1983. Norwich: Unpublished report NCC.
Eastern Daily Press October, 2013. Update: Fish die after salt tides surge up river towards the Norfolk Broads. Retrieved from: http://www.edp24.co.uk/news/update-fish-die-after-salt-tides-surge-up-river-towards-the-norfolk-broads-1-2875787
Ellis, M.B. 1944. The Norfolk Sea Floods February, 1983 2. Detailed observations on the flora at Horsey, 1939. *Transactions of the Norfolk and Norwich Naturalists' Society*, 15, 34-39
England, N. 2009. Responding to the impacts of climate change on the natural environment: The Broads. *Natural England report NE114*.
Espinosa, M. A. 1994. Diatom paleoecology of the Mar Chiquita lagoon delta, Argentina. *Journal of Paleolimnology,* 10**,** 17-23.
Ganning, B. 1971. On the ecology of *Heterocypris salinus, H. incongruens* and *Cypridopsis aculeata* (Crustacea: Ostracoda) from Baltic brackish-water rockpools. *Marine Biology,* 8**,** 271-279.
García-Rodríguez, F., Metzeltin, D., Sprechmann, P., Trettin, R., Stams, G. & Beltrán-Morales, L. F. 2004. Upper Pleistocene and Holocene paleosalinity and trophic state changes in relation to sea level variation in Rocha Lagoon, southern Uruguay. *Journal of Paleolimnology,* 32**,** 117-135.
Geiger,W. 1990. The role of oxygen in the distribution and recovery of the *Cytherissa lacustris* population of Mondsee (Austria). In D.L. Danielopol, P. Carbonel & J.P. Colin (Eds), *Cytherissa (Ostracoda) – the Drosophila of Paleolimnology*, Bulletin de l'Institut de Géologie du Bassin d'Aquitaine, 47/48, 167– 189.

Gell, P. A., Sluiter, I. R. & Fluin, J. 2002. Seasonal and interannual variations in diatom assemblages in Murray River connected wetlands in north-west Victoria, Australia. *Marine and Freshwater Research,* 53**,** 981-992.
George, M. 1992. *Land use, ecology and conservation of Broadland*, Packard Pub.
Gouramanis, C. 2020. Chapter 13 - Ostracoda in extreme-wave deposits. *In:* Engel, M., Pilarczyk, J., May, S. M., Brill, D. & Garrett, E. (eds.) *Geological Records of Tsunamis and Other Extreme Waves.* Amsterdam: Elsevier.
Greaves, M., Caillon, N., Rebaubier, H., Bartoli, G., Bohaty, S., Cacho, I., Clarke, L., Cooper, M., Daunt, C., Delaney, M., Demenocal, P., Dutton, A., Eggins, S., Elderfield, H., Garbe-Schoenberg, D., Goddard, E., Green, D., Groeneveld, J., Hastings, D., Hathorne, E., Kimoto, K., Klinkhammer, G., Labeyrie, L., Lea, D. W., Marchitto, T., Martínez-Botí, M. A., Mortyn, P. G., Ni, Y., Nuernberg, D., Paradis, G., Pena, L., Quinn, T., Rosenthal, Y., Russell, A., Sagawa, T., Sosdian, S., Stott, L., Tachikawa, K., Tappa, E., Thunell, R. & Wilson, P. A. 2008. Interlaboratory comparison study of calibration standards for foraminiferal Mg/Ca thermometry. *Geochemistry, Geophysics, Geosystems,* 9.
Griffiths, H. I. 1995. European Quaternary freshwater Ostracoda: a biostratigraphic and palaeobiogeographic primer. *Scopolia,* 34**,** 1-168.
Hayman, S. 2012. Eccles to Winterton on Sea Coastal Defences. Environment Agency Report to Broads AuthortiyAuthority.
Hayward, C. 2011. High spatial resolution electron probe microanalysis of tephras and melt inclusions without beam-induced chemical modification. *The Holocene,* 22**,** 119-125.
Heip, C. 1976. The life-cycle of *Cyprideis torosa* (Crustacea, Ostracoda). *Oecologia,* 24**,** 229-245.
Henderson, P. 1990. *Freshwater Ostracods*. (Synopses of the British fauna [new series] No. 42). Backhuys, Leiden.
Herbert, E. R., Boon, P., Burgin, A. J., Neubauer, S. C., Franklin, R. B., Ardón, M., Hopfensperger KN, Lamers LP, & Gell, P. 2015. A global perspective on wetland salinization: ecological consequences of a growing threat to freshwater wetlands. *Ecosphere*, *6*(10), 1-43.
Hiller, D. 1972. Untersuchungen zur Biologie und zur Ökologie limnischer Ostracoden aus der Umgebung von Hamburg. *Archiv für Hydrobiologie*, Supplement-Band 40 (4), 400-497.
Holman, I. P., & Hiscock, K. M. (1993). Investigation of salinity in the River Thurne Catchment of North-East Norfolk. Anglian Region Operational Investigation OI 535/1/A.
Holmes, J. A., & Chivas, A. R. (2002). Ostracod shell chemistry - overview. In J. A. Holmes & A. R. Chivas (Eds.), *The Ostracoda: applications in Quaternary research* (Vol. 131, pp. 183-204). Washington DC: American Geophysical Union.
Holmes, J., Jones, R., Nicolas Haas, J., Mcdermott, F., Molloy, K. & O'connell, M. 2007. Multi-proxy evidence for Holocene lake-level and salinity changes at An Loch Mór, a coastal lake on the Aran Islands, Western Ireland. *Quaternary Science Reviews,* 26**,** 2438-2462.
Holmes, J., Sayer, C. D., Liptrot, E. & Hoare, D. J. 2010. Complex controls on ostracod palaeoecology in a shallow coastal brackish-water lake: implications for palaeosalinity reconstruction. *Freshwater Biology,* 55**,** 2484-2498.
Horne, D. (1983). Life-cycles of podocopid Ostracoda-a review (with particular reference to marine and brackish-water species). In R. F. Maddocks (Ed.), *Applications of Ostracoda* (pp. 238-249). Houston: University of Houston.
Horton, B. 1999. The distribution of contemporary intertidal foraminifera at Cowpen Marsh, Tees Estuary, UK: implications for studies of Holocene sea-level changes. *Palaeogeography, Palaeoclimatology, Palaeoecology,* 149**,** 127-149.
Housley, R., Blockley, S., Matthews, I., Macleod, A., Lowe, J., Ramsay, S., Miller, J. & Campbell, E. 2010. Late Holocene vegetation and palaeoenvironmental history of the Dunadd area, Argyll, Scotland: chronology of events. *Journal of Archaeological Science,* 37**,** 577-593.
Juggins S. (2020). *rioja: Analysis of Quaternary Science Data*. R package version 0.9-26, https://cran.r-project.org/package=rioja.
Keatings, K. W., Heaton, T. H. E. & Holmes, J. A. 2002. Carbon and oxygen isotope fractionation in non-marine ostracods: Results from a 'natural culture' environment. *Geochimica et Cosmochimica Acta,* 66**,** 1701-1711.

Kindleysides, D. 1993. *The flooding of the Cantley level in 1993: Monitoring the effects of saline inundation on the aquatic dyke flora in an area of Broadland Grazing Marsh*. Norwich: Report to English Nature

Lane, C. S., Cullen, V. L., White, D., Bramham-Law, C. W. F. & Smith, V. C. 2014. Cryptotephra as a dating and correlation tool in archaeology. *Journal of Archaeological Science,* 42**,** 42-50.

Lane, C. S., Hildebrandt, B., Kennedy, L. M., Leblanc, A., Liu, K.-B., Wagner, A. J. & Hawkes, A. D. 2017. Verification of tropical cyclone deposits with oxygen isotope analyses of coeval ostracod valves. *Journal of Paleolimnology,* 57**,** 245-255.

Larsen, G., Dugmore, A. & Newton, A. 1999. Geochemistry of historical-age silicic tephras in Iceland. *The Holocene,* 9**,** 463-471.

Liu, K.-B., Mccloskey, T. A., Bianchette, T. A., Keller, G., Lam, N. S. N., Cable, J. E. & Arriola, J. 2014. Hurricane Isaac storm surge deposition in a coastal wetland along Lake Pontchartrain, southern Louisiana. *Journal of Coastal Research***,** 266-271.

Löffler, H. 1990. Paleolimnology of Neusiedlersee, Austria. I. The succession of ostracods. *Hydrobiologia,* 214**,** 229-238.

Lowe, J., Gregory, J. M., & Flather, R. 2001. Changes in the occurrence of storm surges around the United Kingdom under a future climate scenario using a dynamic storm surge model driven by the Hadley Centre climate models. *Climate dynamics, 18*(3-4), 179-188.

Marco-Barba, J., Ito, E., Carbonell, E. & Mesquita-Joanes, F. 2012. Empirical calibration of shell chemistry of *Cyprideis torosa* (Jones, 1850) (Crustacea: Ostracoda). *Geochimica et Cosmochimica Acta,* 93**,** 143-163.

Meisch, C. & Broodbakker, B. 1993. *Freshwater Ostracoda (Crustacea) collected by Prof. J.H. Stock on the Canary and Cape Verde islands. With an annotated checklist of the freshwater Ostracoda of the Azores, Madeira, the Canary, the Selvagens and Cape Verde islands. Ostracoda.* Luxembourg: Travaux Scientifiques du Musée National d'Histoire naturelle de Luxembourg.

Meisch, C. 2000. *Freshwater Ostracoda of western and central Europe,* Stuttgart: Gustav Fischer.

Mosby, J.E.G. 1939. The Horsey Flood, 1938: An example of storm effect on a low coast. *The Geographical Journal*, *93*, 413-418.

Murray, J. W. 1979. *British nearshore foraminiferids*, Published for the Linnean Society of London and the Estuarine and Brackish-water Sciences Association by Academic Press.

Neale, J. W. (1988). Ostracods and palaeosalinity reconstruction. In P. De Deckker, J.-P. Colin & J.-P. Peypouquet (Eds.) *Ostracoda in the earth sciences* (125-155). Amsterdam: Elsevier.

Neale, J.W. and Delorme, L.D., 1985. *Cytheromorpha fuscata*, a relict Holocene marine ostracod from freshwater inland lakes of Manitoba, Canada. *Revista Española de Micropaleontologia*, *17*(1), pp.41-64.

Nicholls, R. & Wilson, T. 2001. Integrated impacts on coastal areas and river flooding. *Regional Climate Change Impact and Response Studies in East Anglia and North West England (RegIS). Oxford, UK: UK Climate Impacts Programme (UKCIP)***,** 54-103.

Palmer, S. E., Burn, M. J. & Holmes, J. 2020. A multiproxy analysis of extreme wave deposits in a tropical coastal lagoon in Jamaica, West Indies. *Natural Hazards,* 104**,** 2531-2560.

Park, L. E., Siewers, F. D., Metzger, T. & Sipahioglu, S. 2009. After the hurricane hits: Recovery and response to large storm events in a saline lake, San Salvador Island, Bahamas. *Quaternary International,* 195**,** 98-105.

Patmore, I. R., Sayer, C. D., Goldsmith, B., Davidson, T. A., Rawcliffe, R. & Salgado, J. 2014. Big Ben: a new wide-bore piston corer for multi-proxy palaeolimnology. *Journal of Paleolimnology,* 51**,** 79-86.

Prichard, B. 2013. The North Sea surge and east coast floods of 1953. *Weather, 68*, 31-36.

Rea, H. A., Swindles, G. T. & Roe, H. M. 2012. The Hekla 1947 tephra in the north of Ireland: regional distribution, concentration and geochemistry. *Journal of Quaternary Science,* 27**,** 425-431.

Reid, M., Fluin, J., Ogden, R., Tibby, J. & Kershaw, P. 2002. Long-term perspectives on human impacts on floodplain–river ecosystems, Murray–Darling Basin, Australia. *Internationale Vereinigung für theoretische und angewandte Limnologie: Verhandlungen,* 28**,** 710-716.

Roberts, L. R., Sayer, C. D., Hoare, D., Tomlinson, M., Holmes, J. A., Horne, D. J. & Kelly, A. 2019. The role of monitoring, documentary and archival records for coastal shallow lake management. *Geo: Geography and Environment,* 6 (2), e00083.

Roberts, L.R., Holmes, J.A, Leng, M.J., Sloane, H. & Horne, D.J. 2018. Effects of cleaning methods upon preservation of stable isotopes and trace elements in shells of *Cyprideis torosa* (Crustacea, Ostracoda): Implications for palaeoenvironmental reconstruction. *Quaternary Science Reviews,* 189**,** 197-209.

Rose, N. & Appleby, P. 2005. Regional applications of lake sediment dating by spheroidal carbonaceous particle analysis I: United Kingdom. *Journal of Paleolimnology,* 34**,** 349-361.

Rose, N. L. 1994. A note on further refinements to a procedure for the extraction of carbonaceous fly-ash particles from sediments. *Journal of Paleolimnology,* 11**,** 201-204.

Rose, N. L., Harlock, S., Appleby, P. G. & Battarbee, R. W. 1995. Dating of Recent Lake-Sediments in the United-Kingdom and Ireland Using Spheroidal Carbonaceous Particle (SCP) Concentration Profiles. *Holocene,* 5**,** 328-335.

Ryves, D. B., Clarke, A. L., Appleby, P. G., Amsinck, S. L., Jeppesen, E., Landkildehus, F. & Anderson, N. J. 2004. Reconstructing the salinity and environment of the Limfjord and Vejlerne Nature Reserve, Denmark, using a diatom model for brackish lakes and fjords. *Canadian Journal of Fisheries and Aquatic Sciences,* 61**,** 1988-2006.

Saunders, K. M. 2011. A diatom dataset and diatom-salinity inference model for southeast Australian estuaries and coastal lakes. *Journal of Paleolimnology,* 46**,** 525-542.

Savov, I. P., Luhr, J. F. & Navarro-Ochoa, C. 2008. Petrology and geochemistry of lava and ash erupted from Volcán Colima, Mexico, during 1998–2005. *Journal of Volcanology and Geothermal Research,* 174**,** 241-256.

Spencer, T., Brooks, S. M., Evans, B. R., Tempest, J. A. & Möller, I. 2015. Southern North Sea storm surge event of 5 December 2013: water levels, waves and coastal impacts. *Earth-Science Reviews,* 146**,** 120-145.

Swindles, G. T., Galloway, J. M., Macumber, A. L., Croudace, I. W., Emery, A. R., Woulds, C., Bateman, M. D., Parry, L., Jones, J. M., Selby, K., Rushby, G. T., Baird, A. J., Woodroffe, S. A. & Barlow, N. L. M. 2018. Sedimentary records of coastal storm surges: Evidence of the 1953 North Sea event. *Marine Geology,* 403**,** 262-270.

Tibby, J., Gell, P. A., Fluin, J. & Sluiter, I. R. 2007. Diatom–salinity relationships in wetlands: assessing the influence of salinity variability on the development of inference models. *Hydrobiologia,* 591**,** 207-218.

UNESCO. 1983. Algorithms for computation of fundamental properties of seawater. UNESCO technical papers in marine science, 44, 1–55.

Usskilat, F. 1975. Untersuchungen am Oligohalinikum der Schlei: 2. Über die Ostracodengemeinschaf- ten des Haddebyer und Selker Noores (Schlei). - Kieler Meeresforschungen 31 (2), 151-178.

Vincent, J. 1941. Wild bird protection in Norfolk in 1940 – Notes from Hickling. Transactions of the Norfolk and Norwich Naturalists' Society, 15, 181–184.

Von Grafenstein, U., Erlernkeuser, H. & Trimborn, P. 1999. Oxygen and carbon isotopes in modern fresh-water ostracod valves: assessing vital offsets and autecological effects of interest for palaeoclimate studies. *Palaeogeography Palaeoclimatology Palaeoecology,* 148**,** 133-152.

Weisse, R., Von Storch, H., Niemeyer, H. D. & Knaack, H. 2012. Changing North Sea storm surge climate: An increasing hazard? *Ocean & Coastal Management,* 68**,** 58-68.

Witkowski, A., Cedro, B., Dobosz, S., Seddon, A. W., & Kierzek, A. (2017). Late glacial to Holocene environmental changes (with particular reference to salinity) in the southern Baltic reconstructed from shallow water lagoon sediments. In J. Harff, K. Furmańczyk, H. von Storch (Eds.) *Coastline Changes of the Baltic Sea from South to East* (pp. 175-192). Cham: Spinger.

Woth, K., Weisse, R. & Von Storch, H. 2005. Dynamical Modelling of North Sea Storm Surge Extremes Under Climate Change Conditions: An Ensemble Study. GKSS-Forschungszentrum Geesthacht GmbH, Geesthacht(FRG).

Wouters, K. 1984. Contributions to the study of Belgian Ostracoda. 2. *Cypria subsalsa* Redeke, 1936, in Belgium, with a redescription of the species. *Bulletin d'Institut royal des Sciences naturelle de Belgique, Biologie,* 55 (10), 7 pp, 2 pls.

Xia, J., Ito, E. & Engstrom, D. R. 1997. Geochemistry of ostracode calcite: Part 1. An experimental determination of oxygen isotope fractionation. *Geochimica et Cosmochimica Acta,* 61**,** 377-382.

Yassini, I. 1969. Ecologie des Associations d'Ostracodes du Bassin de l'Arcachon et du Littoral Atlantique. *Bulletin de l'Institut de Géologie du Bassin d'Aquitaine* 7: 1-288; I-XXIV

Yeghicheyan, D., Carignan, J., Valladon, M., Le Coz, M. B., Le Cornec, F., Castrec-Rouelle, M., Robert, M., Aquilina, L., Aubry, E. & Churlaud, C. 2001. A compilation of silicon and thirty-one trace elements measured in the natural river water reference material SLRS-4 (NRC-CNRC). *Geostandards newsletter,* 25**,** 465-474.

Statements and Declarations

Funding

The research was funded by a studentship from the UK Natural Environment Research Council as part of the London NERC DTP (NE/L002485/1) and a CASE partnership with the Broads Authority.

Competing interests

The authors have no relevant financial or non-financial interests to disclose.

Author contributions

Lucy Roberts: Conceptualization, formal analysis, visualization, investigation, writing – original draft. **Jonathan Holmes**: Conceptualization, methodology, supervision, writing - review & editing. **David Horne**: Conceptualization, supervision, writing - review & editing. **Melanie Leng**: Investigation, writing - review & editing**. Carl Sayer**: Conceptualization, supervision, writing - review & editing. **Rhys Timms**: Investigation, writing – review & editing. **Katy Flowers**: Investigation, writing – review & editing. **Simon Blockley**: Formal analysis, visualization, writing – review & editing. **Andrea Kelly**: Conceptualization, supervision, writing – review & editing

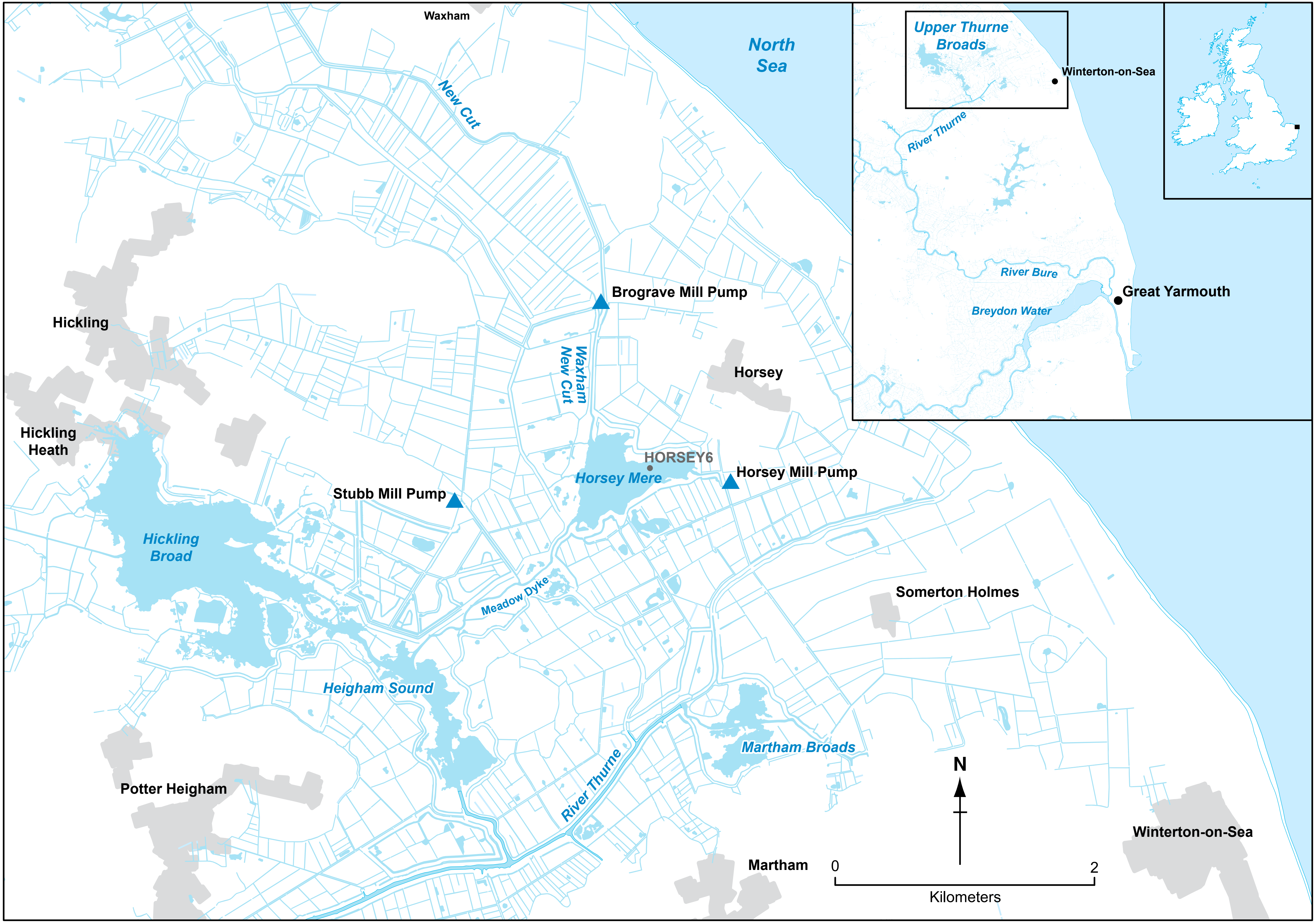

Waxham
North Sea
New Cut
Brograve Mill Pump
Hickling
Waxham New Cut
Horsey
Hickling Heath
HORSEY6
Horsey Mill Pump
Horsey Mere
Stubb Mill Pump
Hickling Broad
Meadow Dyke
Somerton Holmes
Heigham Sound
Martham Broads
Potter Heigham
River Thurne
N
Winterton-on-Sea
Martham
0
2
Kilometers
Upper Thurne Broads
Winterton-on-Sea
River Thurne
River Bure
Great Yarmouth
Breydon Water

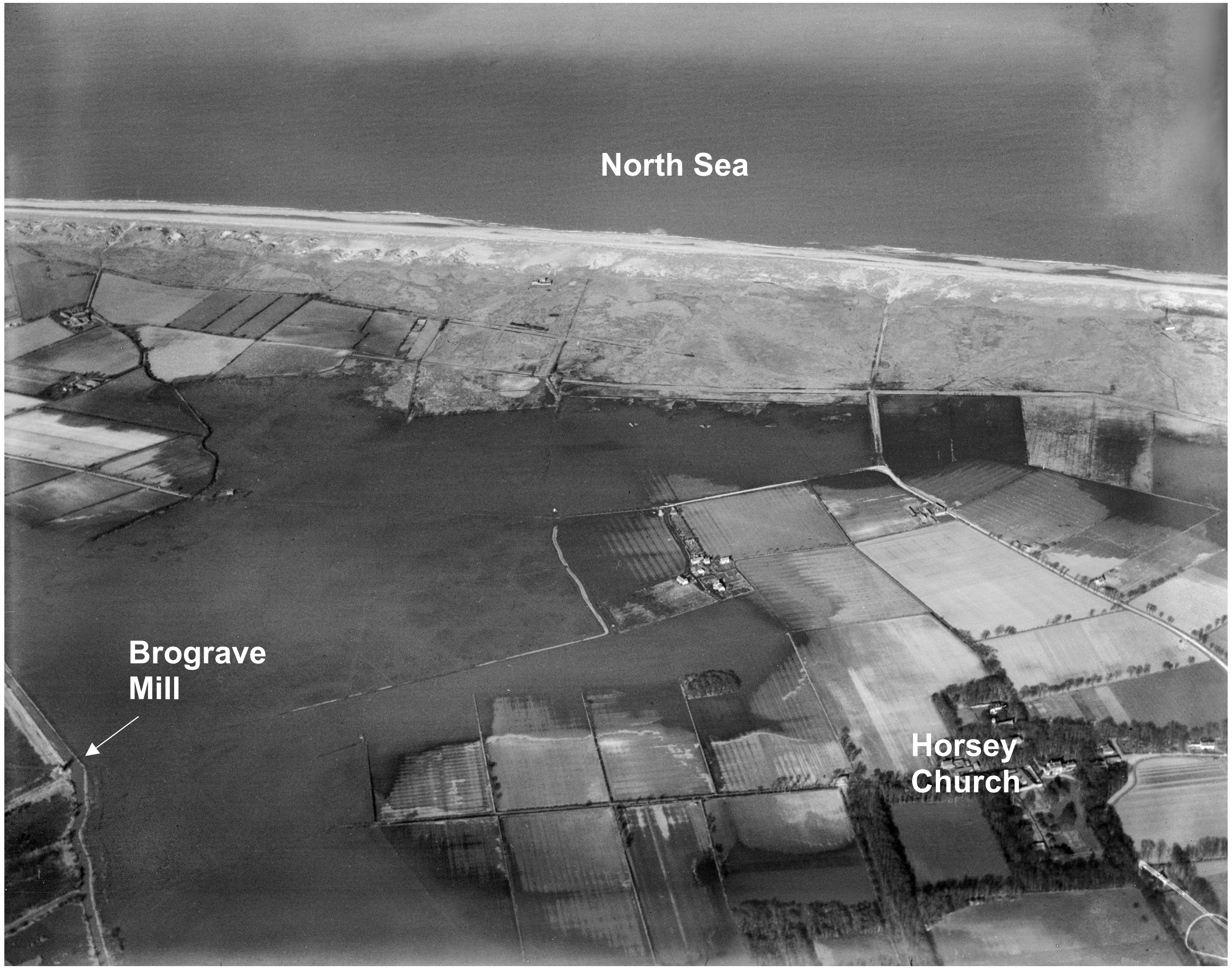
North Sea
Brograve
Mill
Horsey
Church

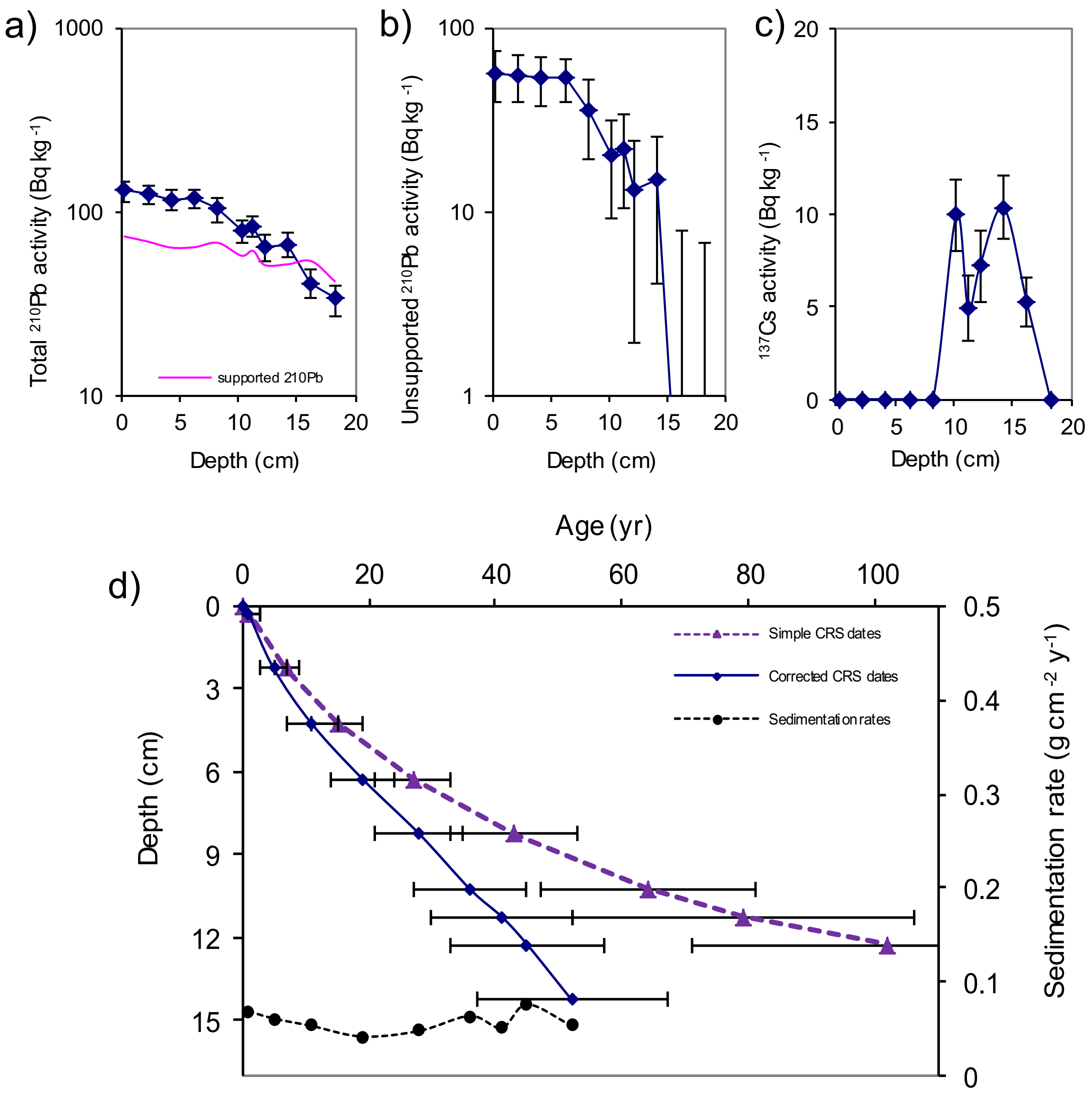

a)
1000
100
10
0
5
10
15
20
Total ^{210}Pb activity (Bq kg^{-1})
Depth (cm)
supported 210Pb
b)
100
10
1
Unsupported ^{210}Pb activity (Bq kg^{-1})
Depth (cm)
c)
20
15
10
5
0
^{137}Cs activity (Bq kg^{-1})
Depth (cm)
Age (yr)
d)
0
20
40
60
80
100
0
3
6
9
12
15
Depth (cm)
0.5
0.4
0.3
0.2
0.1
0
Sedimentation rate (g cm^{-2} y^{-1})
Simple CRS dates
Corrected CRS dates
Sedimentation rates

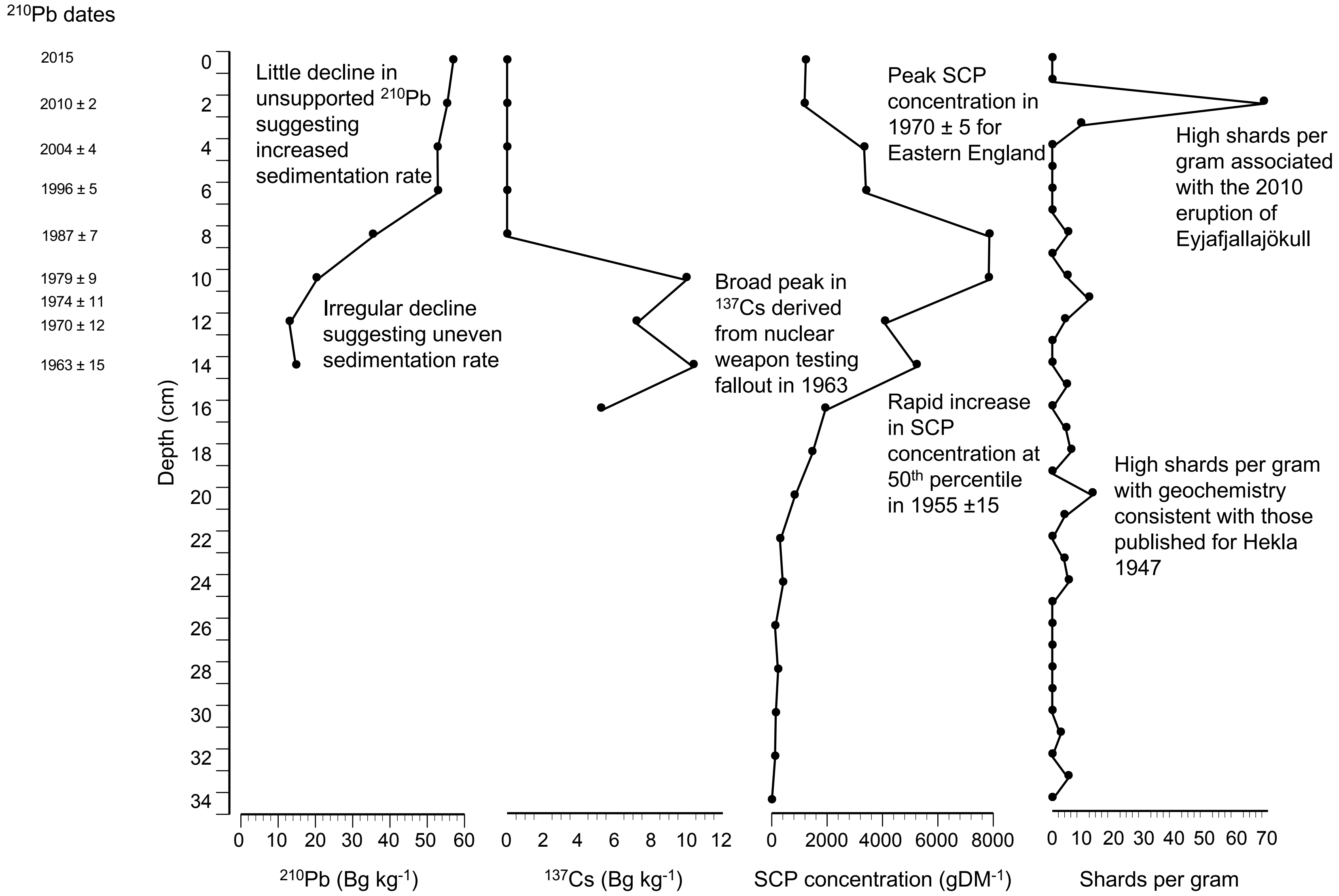

210Pb dates
2015
2010 ± 2
2004 ± 4
1996 ± 5
1987 ± 7
1979 ± 9
1974 ± 11
1970 ± 12
1963 ± 15
Depth (cm)
0
2
4
6
8
10
12
14
16
18
20
22
24
26
28
30
32
34
Little decline in unsupported 210Pb suggesting increased sedimentation rate
Irregular decline suggesting uneven sedimentation rate
Broad peak in 137Cs derived from nuclear weapon testing fallout in 1963
Peak SCP concentration in 1970 ± 5 for Eastern England
Rapid increase in SCP concentration at 50th percentile in 1955 ±15
High shards per gram associated with the 2010 eruption of Eyjafjallajökull
High shards per gram with geochemistry consistent with those published for Hekla 1947
0 10 20 30 40 50 60
0 2 4 6 8 10 12
0 2000 4000 6000 8000
0 10 20 30 40 50 60 70
210Pb (Bg kg-1)
137Cs (Bg kg-1)
SCP concentration (gDM-1)
Shards per gram

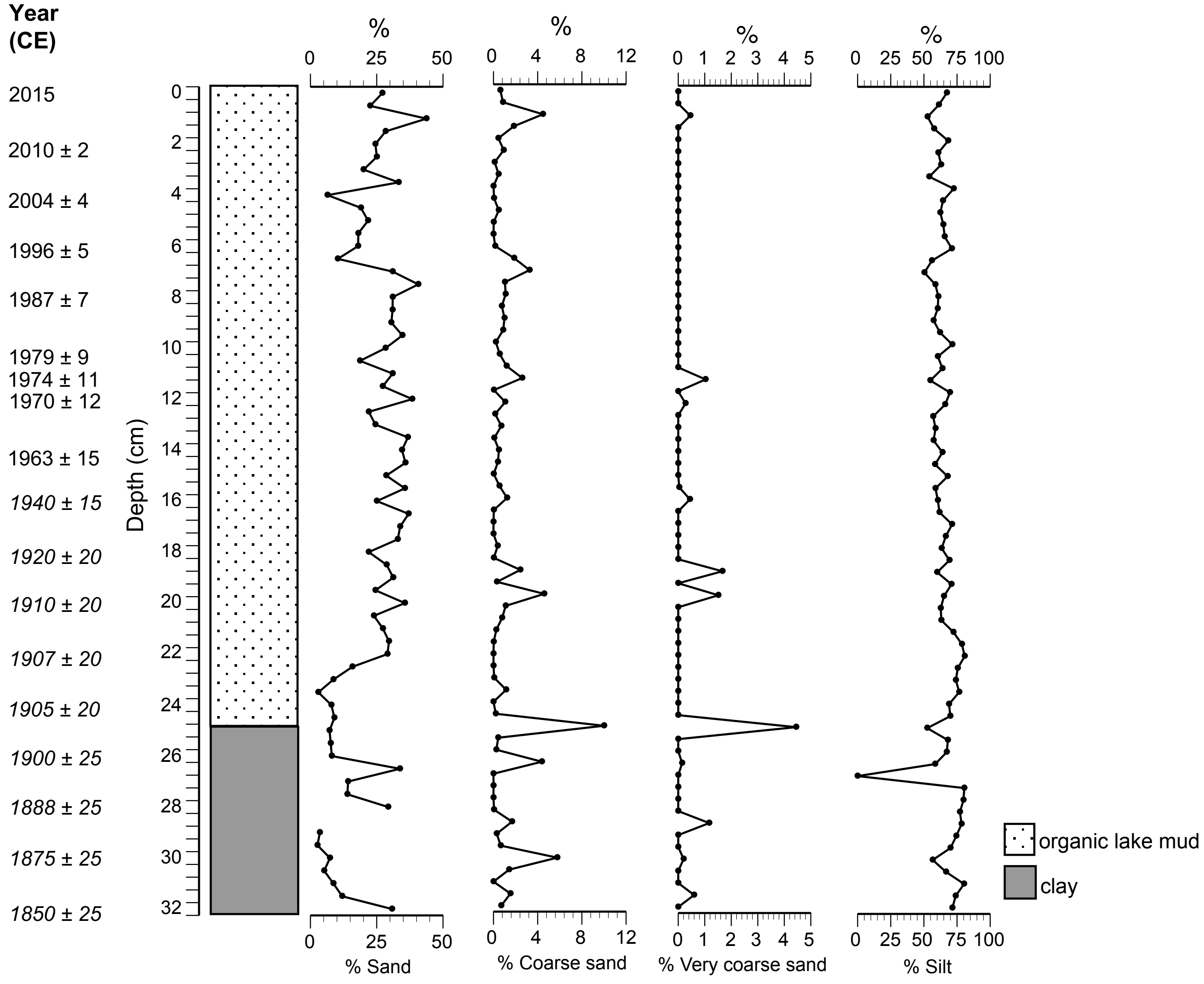

Year (CE)
2015
2010 ± 2
2004 ± 4
1996 ± 5
1987 ± 7
1979 ± 9
1974 ± 11
1970 ± 12
1963 ± 15
1940 ± 15
1920 ± 20
1910 ± 20
1907 ± 20
1905 ± 20
1900 ± 25
1888 ± 25
1875 ± 25
1850 ± 25
Depth (cm)
%
% Sand
% Coarse sand
% Very coarse sand
% Silt
organic lake mud
clay

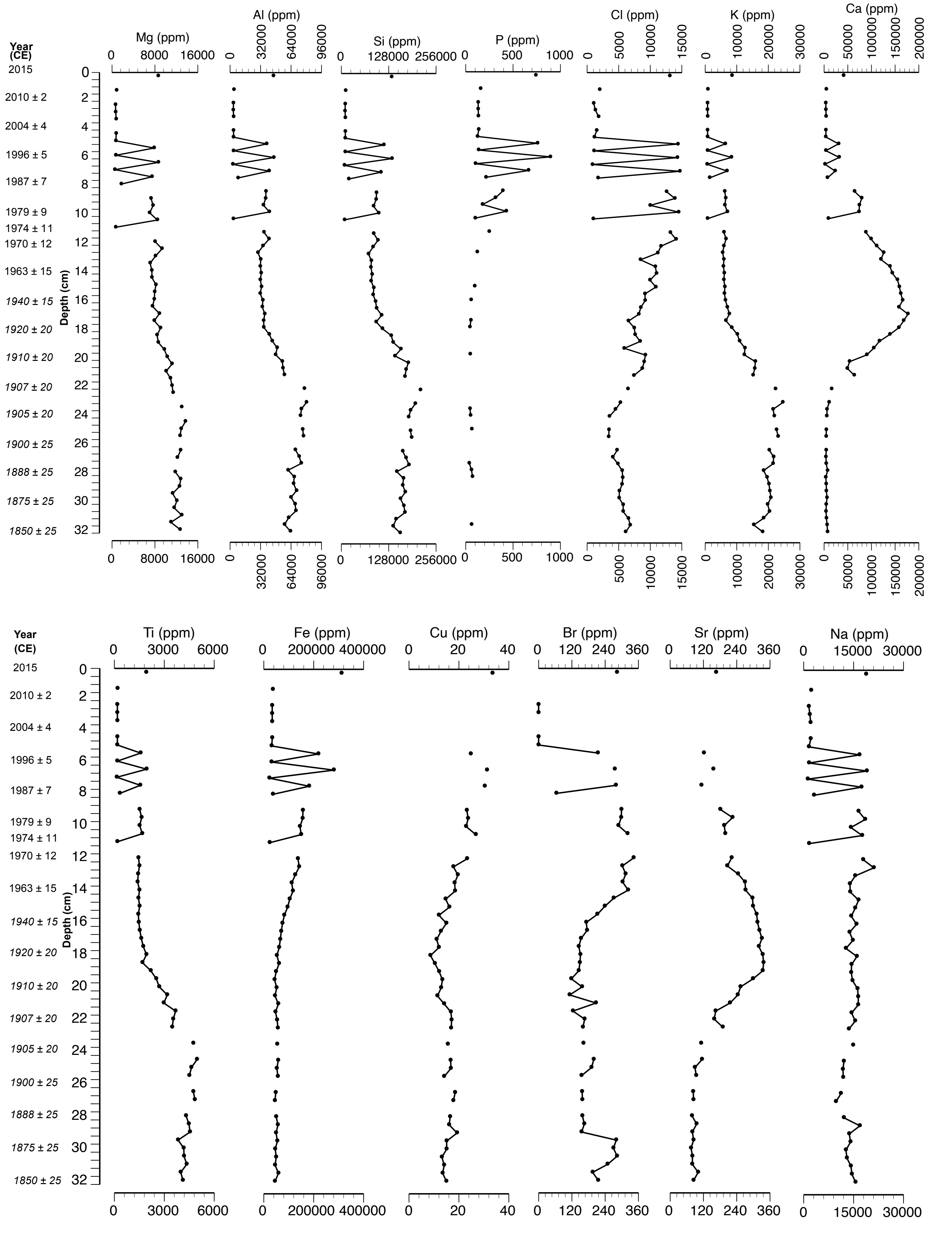
Year (CE)
Depth (cm)
Mg (ppm)
Al (ppm)
Si (ppm)
P (ppm)
Cl (ppm)
K (ppm)
Ca (ppm)
Ti (ppm)
Fe (ppm)
Cu (ppm)
Br (ppm)
Sr (ppm)
Na (ppm)
2015
2010 ± 2
2004 ± 4
1996 ± 5
1987 ± 7
1979 ± 9
1974 ± 11
1970 ± 12
1963 ± 15
1940 ± 15
1920 ± 20
1910 ± 20
1907 ± 20
1905 ± 20
1900 ± 25
1888 ± 25
1875 ± 25
1850 ± 25

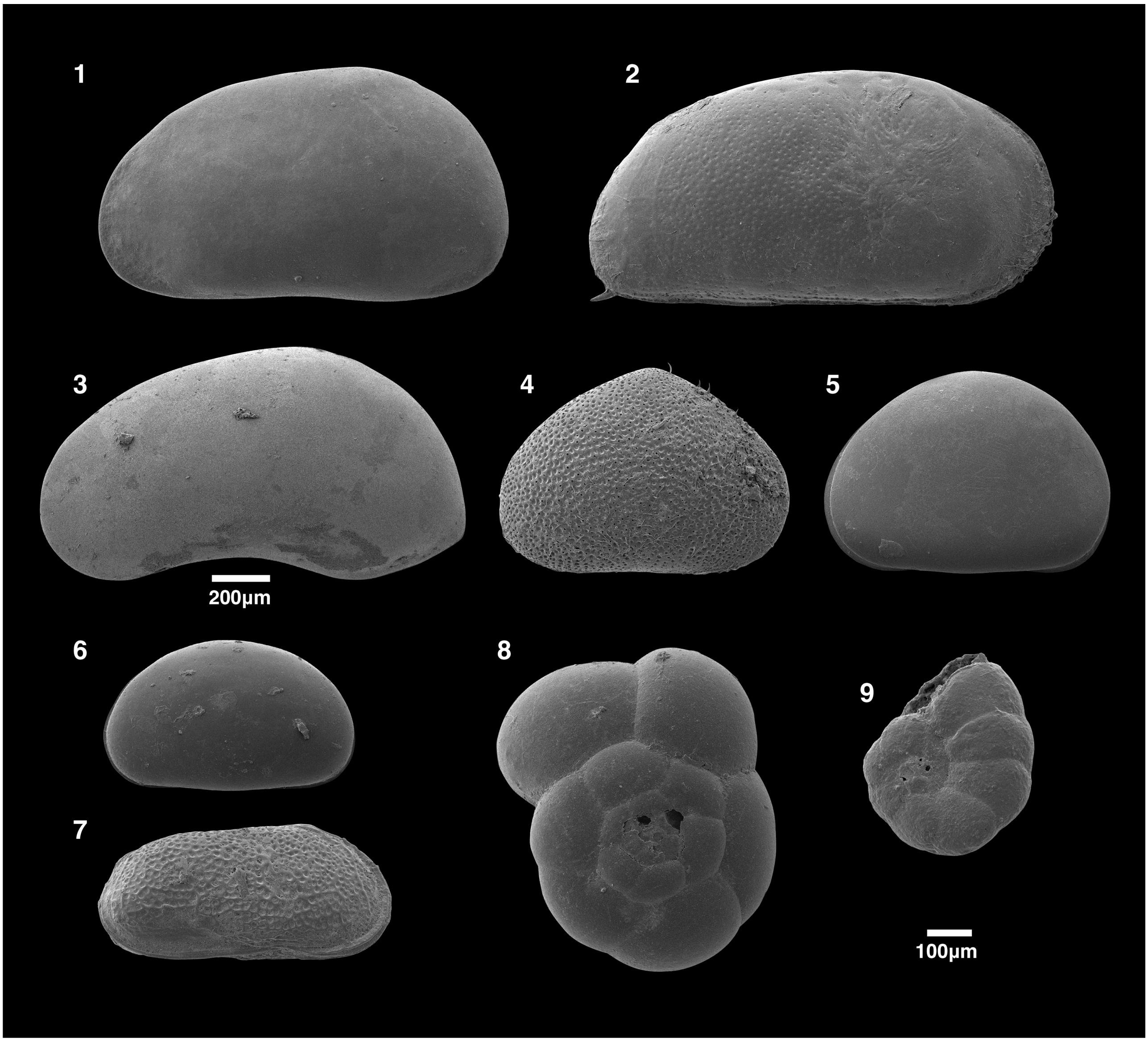
1
2
3
4
5
200µm
6
8
9
7
100µm

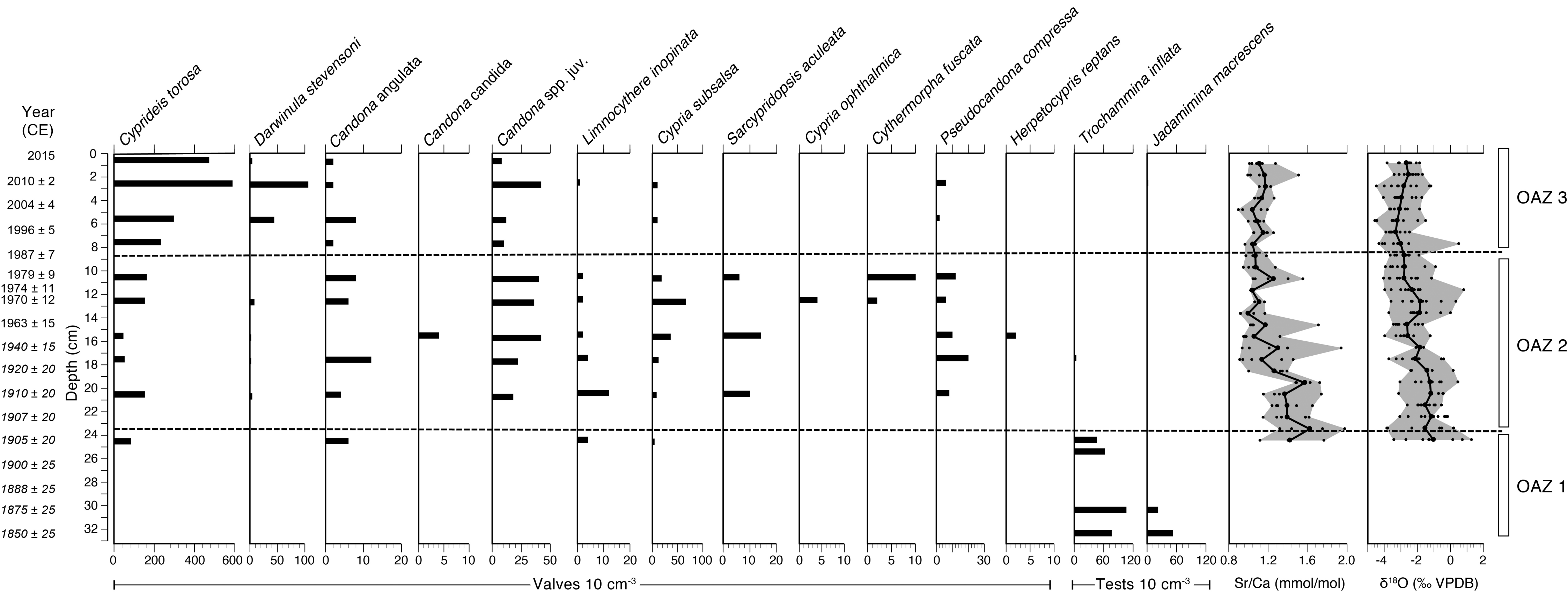

Year (CE)
Depth (cm)
Cyprideis torosa
Darwinula stevensoni
Candona angulata
Candona candida
Candona spp. juv.
Limnocythere inopinata
Cypria subsalsa
Sarcypridopsis aculeata
Cypria ophthalmica
Cythermorpha fuscata
Pseudocandona compressa
Herpetocypris reptans
Trochammina inflata
Jadammina macrescens
Valves 10 cm-3
Tests 10 cm-3
Sr/Ca (mmol/mol)
δ18O (‰ VPDB)
OAZ 3
OAZ 2
OAZ 1
2015
2010 ± 2
2004 ± 4
1996 ± 5
1987 ± 7
1979 ± 9
1974 ± 11
1970 ± 12
1963 ± 15
1940 ± 15
1920 ± 20
1910 ± 20
1907 ± 20
1905 ± 20
1900 ± 25
1888 ± 25
1875 ± 25
1850 ± 25

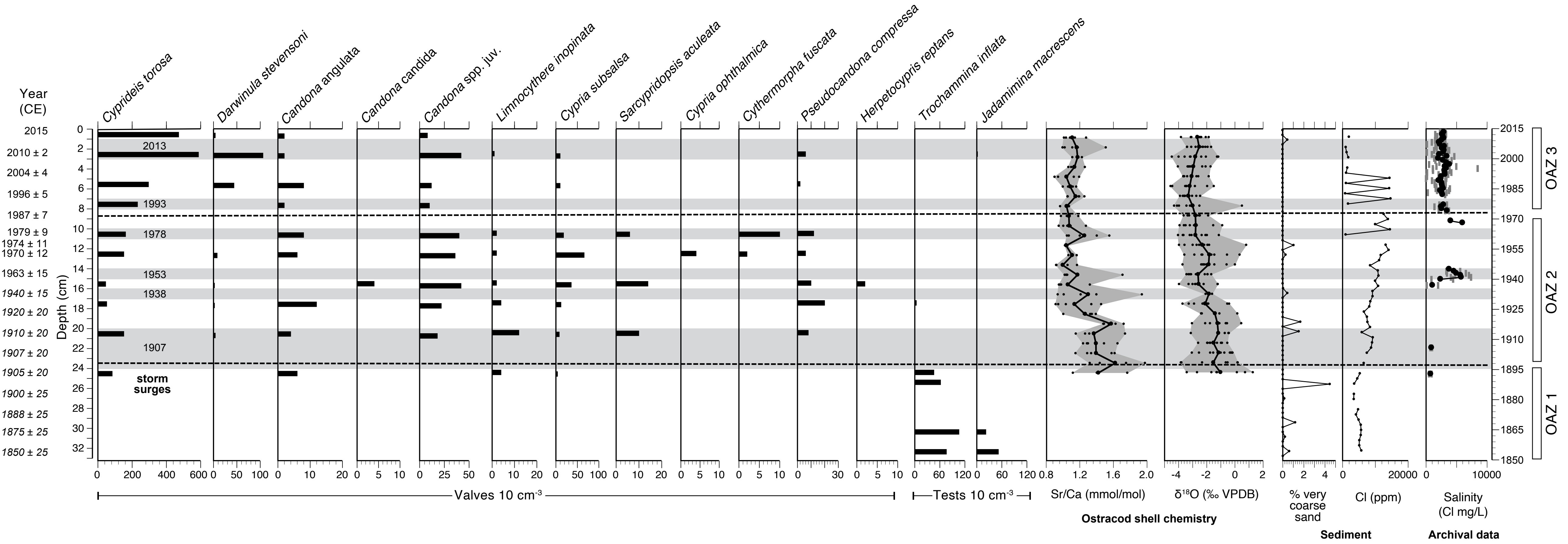

Year (CE)
Depth (cm)
2015
2010 ± 2
2004 ± 4
1996 ± 5
1987 ± 7
1979 ± 9
1974 ± 11
1970 ± 12
1963 ± 15
1940 ± 15
1920 ± 20
1910 ± 20
1907 ± 20
1905 ± 20
1900 ± 25
1888 ± 25
1875 ± 25
1850 ± 25
Cyprideis torosa
Darwinula stevensoni
Candona angulata
Candona candida
Candona spp. juv.
Limnocythere inopinata
Cypria subsalsa
Sarcypridopsis aculeata
Cypria ophthalmica
Cythermorpha fuscata
Pseudocandona compressa
Herpetocypris reptans
Trochammina inflata
Jadamimina macrescens
2013
1993
1978
1953
1938
1907
storm surges
Valves 10 cm⁻³
Tests 10 cm⁻³
Sr/Ca (mmol/mol)
δ18O (‰ VPDB)
Ostracod shell chemistry
% very coarse sand
Cl (ppm)
Sediment
Salinity (Cl mg/L)
Archival data
OAZ 3
OAZ 2
OAZ 1

Reconstruction of short-term storm surge-driven increases in shallow coastal lake salinity using ostracod shell chemistry

Roberts, L.R.[1,2,3*], Holmes, J.A.[3], Horne D.J.[2], Leng M.J.[4,5], Sayer, C.D.[3], Timms R[6]., Flowers, K[6]., Blockley, S.P.M.[6] and Kelly, A.[7]

[1] Department of Ecoscience, Aarhus University, C. F. Møllers Allé 4-5, 8000 Aarhus, Denmark

[2] School of Geography, Queen Mary University of London, Mile End Road, London, E1 4NS, UK

[3] Environmental Change Research Centre, Department of Geography, University College London, Gower Street, London, WC1E 6BT, UK

[4] National Environmental Isotope Facility, British Geological Survey, Keyworth, Nottingham, NG12 5GG, UK

[5] Centre for Environmental Geochemistry, School of Biosciences, University of Nottingham, Sutton Bonington Campus, Loughborough LE12 5RD, UK

[6]Centre for Quaternary Research, Department of Geography, Royal Holloway, University of London, Egham, Surrey TW20 0EX, UK

[7] Broads Authority, Yare House, 62-64 Thorpe Road, Norwich, NR1 1RY, UK

*Correspondence: l.roberts@ecos.au.dk

Supplementary Information 1. Mixing model between storm precipitation (0 PSU) and Horsey Mere lake water (5.6 PSU). Storm precipitation as the proportion of lake water is calculated for the 2013, 1953, and 1938 storm surges. Monthly rainfall data were recorded at Lowestoft Meteorological Station (Met Office, 2022).

Supplementary Information 2. Total alkali-silica biplot of the HORSEY6 tephra at 20 cm (denoted by crosses) against the data for Icelandic eruptions from Hekla 1947 (denoted by triangles) and Askja 1857 (denoted by circles). Historical Icelandic tephra data are from the University of Edinburgh tephra database (http://www.tephrabase.org)

Supplementary Information 3. Variation plots of tephra chemistry major element oxide concentrations. Chemistry of HORSEY6 tephra is denoted by the green crosses with the red triangles and black dots denoting chemistry of widespread late Holocene tephras (Askja 1875 and Hekla 1947).

Supplementary Information 4. Ostracod and foraminifera faunal count data from HORSEY6

Supplementary Information 1. Mixing model between storm precipitation (0 PSU) and Horsey Mere lake water (5.6 PSU). Storm precipitation as the proportion of lake water is calculated for the 2013, 1953, and 1938 storm surges. Monthly rainfall data were recorded at Lowestoft Meteorological Station (Met Office, 2022).

	Proportion of lake = rain	**Proportion of lake = Horsey Mere lake water**	**PSU of mixture**
Dec 2013	0.03	0.97	5.4
Jan 1953	0.02	0.98	5.5
Feb 1938	0.01	0.99	5.5

Supplementary Information 2. Total alkali-silica biplot of the HORSEY6 tephra at 20 cm (denoted by crosses) against the data for Icelandic eruptions from Hekla 1947 (denoted by triangles) and Askja 1857 (denoted by circles). Historical Icelandic tephra data are from the University of Edinburgh tephra database (http://www.tephrabase.org)

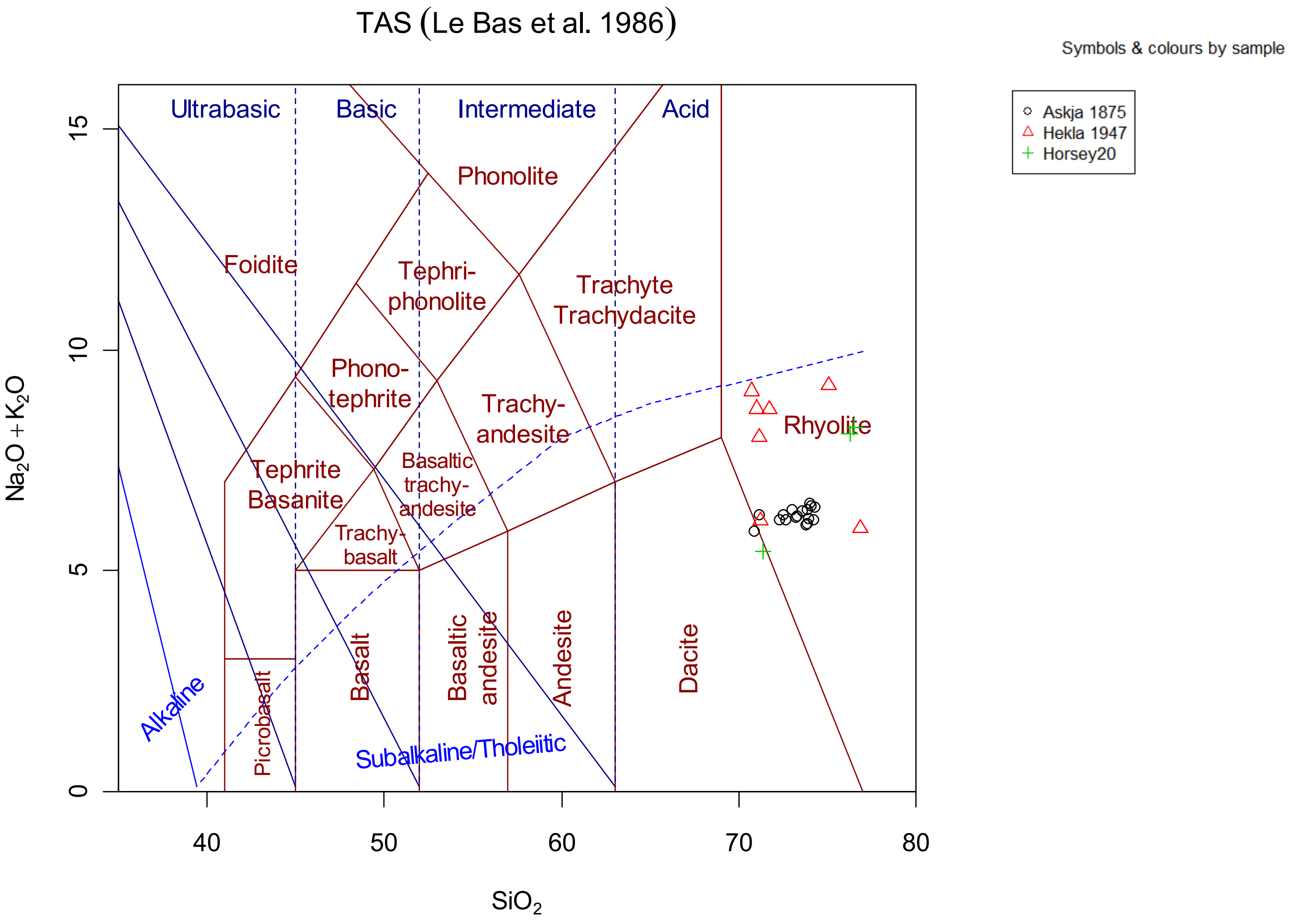

Supplementary Information 3. Variation plots of tephra chemistry major element oxide concentrations. Chemistry of HORSEY6 tephra is denoted by the green crosses with the red triangles and black dots denoting chemistry of widespread late Holocene tephras (Askja 1875 and Hekla 1947).

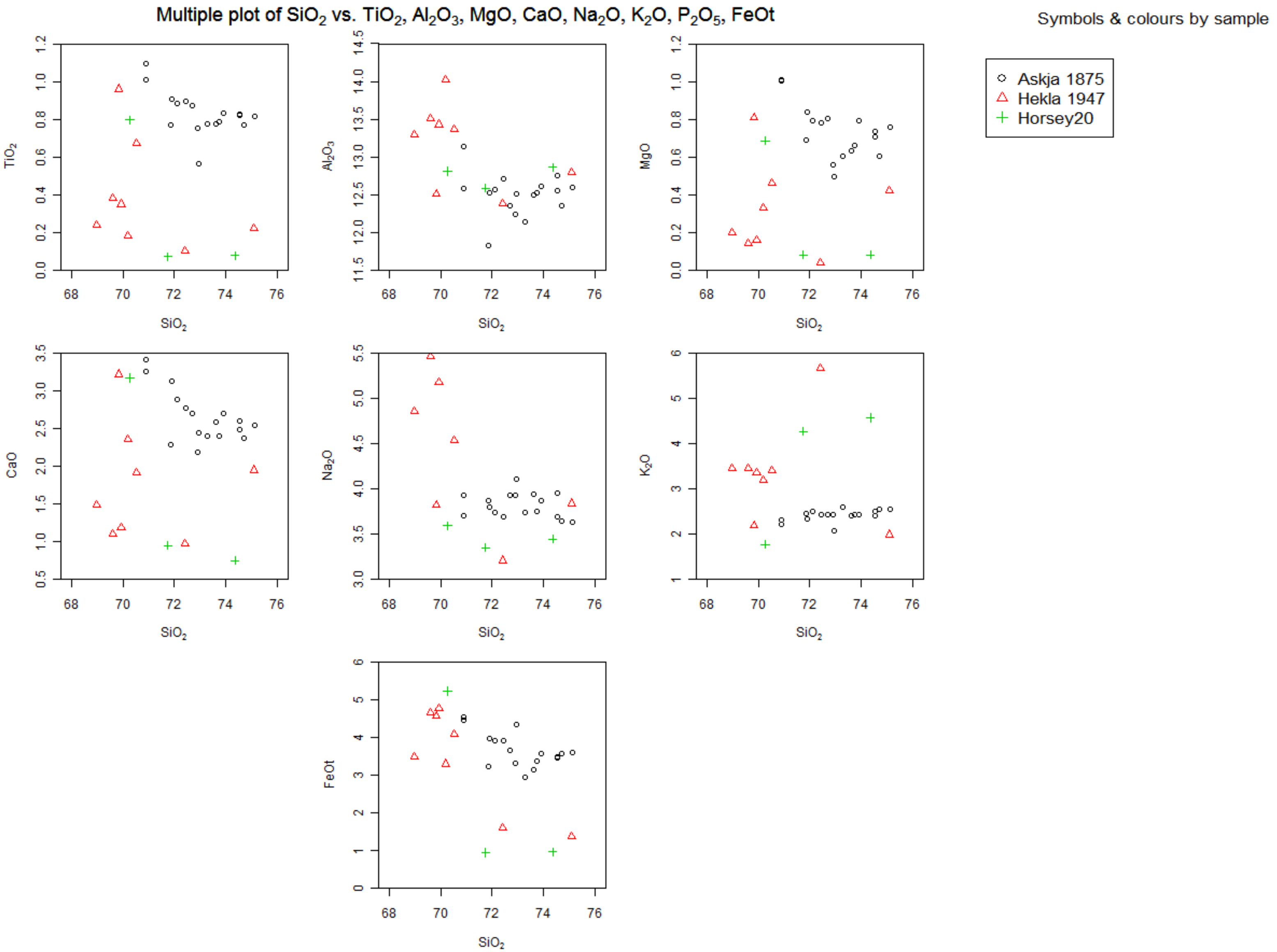

Supplementary Information 4. Ostracod and foraminifera faunal count data from HORSEY6

Depth (cm)	*Cyprideis torosa*	*Darwinula stevensoni*	*Candona angulata*	*Candona candida*	*Candona* spp. juv.	*Limnocythere inopinata*	*Cypria subsalsa*	*Sarscypridopsis aculeata*	*Cypria ophtalmica*	*Cytheromorpha fuscata*	*Pseudocandona compressa*	*Herpetocypris retans*	*Trochammina inflata*	*Jadammina macrescens*
0	236	2	1	0	4	0	0	0	0	0	0	0	0	0
2	294	53	1	0	21	0	5	0	0	0	3	0	0	1
5	148	22	4	0	6	0	5	0	0	0	1	0	0	0
7	116	0	1	0	5	0	0	0	0	0	0	0	0	0
10	81	0	4	0	20	1	9	3	0	5	6	0	0	0
12	76	4	3	0	18	1	33	0	2	1	3	0	0	0
15	23	1	0	2	21	1	18	7	0	0	5	1	0	0
17	26	1	6	0	11	2	6	0	0	0	10	0	2	0
20	76	2	2	0	9	6	4	5	0	0	4	0	0	0
24	42	0	3	0	0	2	2	0	0	0	0	0	23	0
25	3	0	0	0	0	0	0	0	0	0	0	0	31	0
30	0	0	0	0	1	0	0	0	0	0	0	0	53	11
32	0	0	0	0	0	0	0	0	0	0	0	0	38	26